UNIVERSITÀ
DI PAVIA

FACULTY OF ENGINEERING

DEPARTMENT OF CIVIL ENGINEERING
AND ARCHITECTURE

MASTER'S DEGREE IN
ENVIRONMENTAL ENGINEERING
(Resilience to climate change effects)

# Assessment of Climate Change Effects on Low Flow Conditions Using the SWAT Model (Case Study: Serio River)

Supervisor:
**Prof. Giuseppe Barbero**

Co-supervisor:
**Name Surname**

Candidate:
**Azar Sharifiyan kakhki**
**Mat. 519580**

A.Y. 2025/2026

# Abstract

This thesis investigates the impacts of climate change on river discharge and low-flow conditions in the Serio River basin using the SWAT+ hydrological model under the RCP 4.5 scenario. Bias-corrected climate projections were used to simulate future hydrological conditions (2026–2050), which were compared with the baseline period (2014–2025). Model calibration and validation were performed using observed discharge data to ensure reliable representation of basin-scale hydrological processes. Low-flow conditions were assessed using the Q95 index.

The results indicate a clear seasonal shift in low-flow behavior, characterized by increased discharge during winter months and significant reductions during summer. In particular, Q95 values decrease substantially during the dry season, with reductions reaching up to 99% in downstream areas, where discharge approaches near-zero conditions.

A pronounced spatial variability was observed, with the downstream station (Montodine) exhibiting significantly higher vulnerability to low-flow conditions compared to the upstream station (Cene). In addition, future climate conditions are associated with increased interannual variability, leading to more frequent occurrences of extreme low-flow years.

Overall, the findings suggest that climate change will intensify low-flow conditions, increase their variability, and elevate the risk of hydrological drought in the basin. These results highlight the importance of implementing effective water resource management and adaptation strategies under changing climatic conditions.

**Keywords:** Climate change, low flow, SWAT+, hydrological modeling

# Abstract in lingua Italiano

Questa tesi analizza gli effetti del cambiamento climatico sulla portata fluviale e sulle condizioni di magra nel bacino del fiume Serio utilizzando il modello idrologico SWAT+ sotto lo scenario RCP 4.5. Le proiezioni climatiche, opportunamente corrette tramite bias correction, sono state utilizzate per simulare le condizioni idrologiche future (2026–2050), confrontandole con il periodo di riferimento (2014–2025). La calibrazione e la validazione del modello sono state effettuate utilizzando dati osservati di portata al fine di garantire una rappresentazione affidabile dei processi idrologici a scala di bacino. Le condizioni di magra sono state valutate mediante l'indice Q95.

I risultati evidenziano una chiara variazione stagionale nel comportamento delle portate di magra, caratterizzata da un aumento delle portate nei mesi invernali e da una significativa riduzione durante il periodo estivo. In particolare, i valori di Q95 diminuiscono in modo marcato durante la stagione secca, con riduzioni fino al 99% nelle aree a valle, dove la portata tende a valori prossimi allo zero.

È stata inoltre osservata una marcata variabilità spaziale, con la stazione a valle (Montodine) che mostra una vulnerabilità significativamente maggiore alle condizioni di magra rispetto alla stazione a monte (Cene). Inoltre, le condizioni climatiche future sono associate a un aumento della variabilità interannuale, con una maggiore frequenza di anni caratterizzati da portate estremamente basse.

Nel complesso, i risultati indicano che il cambiamento climatico porterà a un'intensificazione delle condizioni di magra, a un aumento della loro variabilità e a un incremento del rischio di siccità idrologica nel bacino. Questi risultati sottolineano l'importanza di strategie efficaci di gestione delle risorse idriche e di misure di adattamento in un contesto climatico in evoluzione.

**Parole chiave:**
Cambiamento climatico, magra, SWAT+, modellazione idrologica,

# Table of Contents

# INTRODUCTION

Climate change is one of the most pressing global challenges affecting water resources and hydrological systems worldwide. Changes in temperature and precipitation patterns have significant impacts on river flow regimes, particularly on low-flow conditions, which are critical for water availability and ecosystem sustainability.

In recent years, increasing attention has been given to assessing the impacts of climate change on river basins using hydrological models. Low-flow conditions, often associated with hydrological droughts, are especially sensitive to climatic variations and represent a key concern for water resource management.

This thesis focuses on the analysis of low-flow conditions in the Serio River basin under climate change scenarios. Using the SWAT+ model and climate projections under the RCP 4.5 scenario, the study evaluates how future conditions may affect river discharge and low-flow conditions, as represented by the Q95 index.

## ACKNOWLEDGEMENTS

I would like to express my sincere gratitude to all those who supported and encouraged me throughout this journey. Their guidance, patience, and understanding were essential during both the challenging and rewarding phases of this work.

I would especially like to thank my supervisor for their invaluable guidance, continuous support, and insightful comments, which greatly contributed to the development of this research.

I am deeply grateful to my family for their constant support, trust, and motivation, which gave me the strength to keep going even in difficult moments.

Finally, I would like to thank my friends and colleagues who shared this path with me, offering help, perspective, and encouragement along the way.

# 1 Chapter 1: STATE OF THE ART

## 1.1 climate change

Climate change is arguably the most severe challenge facing our planet during the 21st century. [1]

Under balance of evidence, global warming is unequivocal and most of it is very likely due to the increase in atmospheric greenhouse gas concentrations. Observed climate change has extended beyond temperature. However, there are multiple pressures of global change, such as: population growth, land use and land cover changes (urbanization, especially in coastal areas, deforestation), and environmental pollution, which in many areas are exacerbated by climate change. [2]

Human interference with the climate system، mainly through the emission of greenhouse gases and changes in land use، has increased the global and annual mean air temperature at the Earth's surface by roughly 0.8 °C since the 19th century.[1]

The Fourth Assessment Report of the Intergovernmental Panel on Climate Change (IPCC, 2007) stated that the global average surface air temperature has increased by 0.74°C during the 20th century, with a more rapid warming trend over the past 50 years. The report indicated that the global average temperature will increase by 1.8°C to 4.0°C by the year 2100 compared to temperatures during 1980-1999. The assessment report also projected that the increased precipitation intensity and variability could increase the risks of flooding and drought in many areas of the globe during the 21st century. [3]

There is broad agreement that a warming of this magnitude would have profound impacts both on the environment and on human societies (IPCC, 2014a), and that climate change mitigation via a transformation to decarbonized economies and societies has to be achieved to prevent the worst of these impacts. There is a wide range of global threats that certainly require humanity's urgent attention (see the recent report by the World Economic Forum, 2015). These global risks include water, food and energy security, opulation growth, infectious diseases, and international security.[1]

## 1.2 Climate & Water (Hydrological link)

Climate and water on the planet Earth are intimately linked. Water influences the climate, and is influenced by the climate. Every change in the climatic system induces a change in the water system, and the other way round. Climate change has been observed and even a stronger change is projected for the future by climate models. Discussion of changes is presented, with reference to such variables as temperature, precipitation, sea level, river flow, soil moisture, evapotranspiration, groundwater, and cryospheric characteristics. The weight of observational evidence indicates an ongoing intensification of the water cycle, with increasing rates of evaporation and precipitation. Climate change will alter the future world's freshwater resources in several aspects, such as freshwater availability, quality, and destructive potential.[2]

Climate change is likely to lead to an intensification of the global hydrological cycle and to have a major impact on regional water resources.[4]

Climate change alters the overall discharge regime of river basins and modifies the stream and base flow in channel systems.[5]

The IPCC Fourth Assessment Report mentions with high likelihood that observed and projected increases in temperature, sea level rise and precipitation variability are the main causes for reported and projected impacts of climate change on water resources, resulting in an overall net negative impact on water availability and the health of freshwater ecosystems.[4]

## 1.3 Climate Change and Hydrological Systems

General circulation models (GCMs) are one of the primary instruments for obtaining projections of future global climate change.[6]

An alternative approach for the estimation of potential changes in the future is the use of climate change projections. When using this approach, one should link several models in order to estimate the potential impact of future changes on the runoff dynamics. The bases are the global circulation models (GCMs) with the Intergovernmental Panel on Climate Change (IPCC) Special Report on Emission Scenarios (SRES) scenarios and the representative concentration pathways (RCP). [7]

The sophistication of GCMs over the past decade has considerably improved their ability to simulate present and past climates.

Despite the advancements in the success of GCMs in simulating past and future climate conditions at global and continental scales, they have inherent limitations in providing the climate features and dynamics at the local scale.

GCMs provide outputs at a resolution that is too coarse for using directly in hydrologic modeling studies.[3]

The GCMs' outputs should be downscaled and bias corrected (BC) before they can potentially be used as an input to the hydrological models.[7]

In order to downscale the outputs of a GCM for regional or local studies, several techniques have been developed, which are broadly classified as statistical downscaling and dynamical downscaling.

Regional climate models (RCMs) use GCM output at their boundaries to dynamically describe land, atmosphere, and water body interactions at finer resolutions in a limited geographical area. RCMs are able to generate the high-resolution meteorological inputs required to conduct climate impact studies at the regional level.

Uncertainty of the outputs derived from RCMs is always a topic of interest for any target region.

The potential climate scenarios are used in hydrologic models, such as the Soil and Water Assessment Tool (SWAT) and Precipitation Runoff Modeling System (PRMS) to study climate impact on the watershed and streamflow. SWAT is widely accepted watershed model for long-term continuous simulation in predominantly agricultural watersheds .This comprehensive model has been successfully applied in many countries all over the world for continuous simulation of flow, for predictions of sediment and nutrient loss, and for evaluating best management practices, as well as for climate change impact studies. [3]

## 1.4 Low Flow in River Systems

International glossary of hydrology defines low flow as 'flow of water in a stream during prolonged dry weather'. This definition does not make a clear distinction between low flows and droughts. Low flows is a seasonal phenomenon, and an integral component of a flow regime of any river. Drought, on the other hand, is a natural event resulting from a less than normal precipitation for an extended period of time. [8]

low flow generally refers to streamflow during prolonged dry weather conditions.

The assessment of low-flow characteristics is important for water resources planning and management, designing water systems, management of environmental flow, conserving aquatic life, as well for water taking permits. Characterization and analysis of low flow are needed for both water users and regulatory authorities .[3]

Accepting the definition of low flow as a period in which the flow is equal to or less than the assumed threshold discharge one should adopt the following steps: define a criterion for determining the threshold discharge,

-separate the low flow as independent events from long time series,

- determine the parameters of low flows,

-classify the low flow parameters, i.e., low flow deficit volume (Di), low flow duration (Ti), in order to separate the extreme hydrological drought likelihood from a set of (Di, Ti).

Criterion for the threshold selection and separation of hydrological droughts from a series of low flow events was following the classification proposed by Dracup et al. (1980). He provides a rough separation between low flow and drought by combining the notion of the truncation level with the averaging period.

The threshold might be, however, chosen in a number of ways and the choice depends on a function of water deficit and the purpose of the study. Hence, the threshold level depends on climatic conditions, availability of data as well as hydrological regime of the river.[9]

A number of natural factors that affect the low-flow regime of a river include topography, infiltration characteristics of soils, hydraulic properties of the aquifers, vegetation cover, and climate.[3]

## 1.5 Factors Influencing Low Flows

Low flows normally stem from groundwater, and the natural processes that drive low flows are the recharge, storage and discharge of groundwater and of lakes or melting glaciers in some regions. Therefore, the factors that influence low flows include the climate, the extent to which aquifers are drained, the characteristics of soils, the subsurface hydraulic properties, the categories of geologic units, and the extent of human interference.[10]

In more detail, the natural factors which influence the various aspects of the low-flow regime of the river include the distribution and infiltration characteristics of soils, the hydraulic characteristics and extent of the aquifers, the rate, frequency and amount of recharge, the evapotranspiration rates from the basin, distribution of vegetation types, topography and climate. These factors and processes may be grouped into those affecting gains and losses to

streamflow during the dry season of the year. Anthropogenic effects on these processes and on the streamflow directly should be considered separately.[8]

## 1.6 Climate Change Impacts on Low Flows

If climate change results in changes of both the intensity and reliability of the monsoon, it will affect both high and low flows leading to increased flooding but possibly also to increased variability of available water, both in space and time.[4]

climate change will likely increase the persistence of both high and low flows due to decreasing snowfall and earlier snowmelt, resulting in an earlier occurrence of snowmelt-induced peaks and drier summers.[11]

There is some evidence that climate change has already affected occurrence of both floods and hydrological droughts in some parts of the world.[12]

Floods and low flows in these rivers may cause several problems to society. Since floods are eye-catching, quick and violent events risking human-life, water authorities often focus on flood issues. In contrast, hydrological droughts, causing low flows, develop slowly and affect a much larger area than floods. Low flows in rivers may negatively affect all important river functions.[11]

# 2 Chapter 2: AIM OF THE WORK

## 2.1 Background

This chapter focuses on reviewing the current understanding of climate change impacts on river flow regimes, with particular emphasis on low-flow conditions. Since low flows represent critical periods of water scarcity, they play an essential role in water resource management, environmental sustainability, and hydrological planning. Therefore, it is important to analyze how climatic variables such as temperature and precipitation influence low-flow behavior.

To achieve this, particular attention is given to studies that have applied hydrological models, especially the Soil and Water Assessment Tool (SWAT), to simulate streamflow under changing climate conditions. These models, often combined with climate projections from General Circulation Models (GCMs) and Regional Climate Models (RCMs), provide a framework for assessing future hydrological responses at the basin scale.

In addition, this chapter considers the methods used to quantify low-flow conditions, including flow duration curves and commonly used indices such as Q90 and Q95. These indices are widely applied to evaluate water availability during dry periods and to assess the severity of low-flow events.

The review also includes studies that address uncertainties related to climate projections, model structures, and downscaling techniques, as these factors significantly influence the reliability of low-flow predictions. Furthermore, attention is given to the role of seasonal variability and catchment characteristics in shaping low-flow dynamics.

Overall, this chapter aims to provide a comprehensive overview of existing approaches and methodologies used to assess climate change impacts on low flows, forming the basis for the analysis carried out in this study.

## 2.2 Climate Change Impacts on Low Flows

### *2.2.1 EFFECT OF CLIMATE CHANGE ON LOW-FLOW CONDITIONS IN THE RUSCOM RIVER WATERSHED, ONTARIO*

Rahman et al. (2010) evaluated the impact of climate change on low-flow conditions in the Ruscom River watershed using SWAT, CRCM, and LARS-WG. The results showed an increase in temperature (≈3–3.6°C) and precipitation (~8%) under future scenarios. Despite this, low flows are projected to decrease during summer and fall due to higher evapotranspiration, while increasing in spring. Flow duration curve analysis indicated that extreme low flows (e.g., 5-

year return period) could decrease by up to 50%. The study highlights the strong influence of seasonal climate variability on low-flow regimes.[3]

### *2.2.2 Impact of climate change on low-flows in the river Meuse*

de Wit et al. (2007) analysed the impact of climate change on low-flow conditions in the Meuse River basin using long-term observations, RCM simulations, and the HBV model. The study identified meteorological drivers of low flows through relationships between precipitation, temperature, and low-flow indices. Results showed that low flows are mainly controlled by multi-seasonal droughts, especially the combination of dry winters and dry summers. Summer precipitation was found to have the strongest influence, while winter precipitation contributes via groundwater recharge. Future projections indicate wetter winters and drier summers, increasing discharge seasonality, without a clear rise in extreme low-flow frequency. Simulations suggest reduced summer discharge, although limitations exist in reproducing critical low-flow events. Overall, the study highlights the complexity of low-flow processes and the role of groundwater and seasonal interactions.[13]

### *2.2.3 Impact of climate change on the stream flow of the lower Brahmaputra: trends in high and low flows based on discharge-weighted ensemble modelling*

This study investigates the impact of climate change on both high and low streamflow in the lower Brahmaputra River using a discharge-weighted ensemble approach. Instead of relying on a single model, the authors combined outputs from 12 global climate models (GCMs) and applied a global hydrological model to simulate future streamflow (1961–2100). The results indicate that extreme low-flow events are likely to become less frequent due to increased precipitation, whereas peak flows are expected to increase significantly, raising flood risks. The study highlights the importance of using multi-model ensembles to reduce uncertainty in climate impact assessments. The proposed methodology also improves the representation of observed discharge by weighting models based on their performance .[4]

## 2.3 Hydrological Modelling Approaches

### *2.3.1 Assessment of Climate Change Impacts on Extreme High and Low Flows: An Improved Bottom-Up Approachv*

In this study, an improved bottom-up approach was proposed to assess climate change impacts on extreme high and low flows. The authors generated large ensembles of climate projections

by combining regional climate models with stochastic weather generators. These projections were then used as inputs to a calibrated SWAT hydrological model to simulate future streamflow. The results were analyzed using probabilistic methods to estimate the likelihood of extreme events. The study demonstrated that the proposed approach provides better coverage of uncertainty and improves risk assessment compared to traditional top-down methods.[14]

### *2.3.2 How will climate change modify river flow regimes in Europe?*

The study by Schneider et al. (2013) examines the impact of climate change on river flow regimes across Europe using the WaterGAP3 model and multiple climate scenarios. Results show that climate change significantly alters flow magnitude and timing, with the strongest impacts in the Mediterranean and boreal regions. A north–south contrast is observed, where northern Europe becomes wetter while southern regions experience reduced precipitation and streamflow. Low flows are projected to decrease in southern and eastern Europe, whereas northern regions may experience increased winter flows due to higher precipitation and earlier snowmelt. Overall, climate change is expected to modify hydrological regimes and increase pressure on water resources and ecosystems.[15]

## 2.4 Low-Flow Characterization and Indices

### *2.4.1 Classification of Low Flow and Hydrological Drought for a River Basin*

This study focuses on the classification of low flows and hydrological droughts in a river basin using quantitative indices. The authors define hydrological drought as a period of sustained water deficit associated with low river flows and propose a methodology based on threshold levels (e.g., Q70%) to identify low-flow events. A key contribution is the introduction of the Hydrological Drought Index (HDI), which combines deficit volume and duration (Di × Ti) to characterize drought severity. Based on this index, drought events are classified into five categories ranging from short-term low flow to extreme hydrological drought. The study also highlights the relationship between hydrological drought and atmospheric conditions, showing strong correlations between climatic water balance and drought occurrence.[9]

### *2.4.2 Analyzing the Impacts of Climatic and Physiographic Factors on Low Flow Distribution*

In this study, the impacts of climatic and physiographic factors on low flow distributions were investigated using a derived distribution function approach. The methodology was based on

the linear recession equation, considering both dry spell duration and recession response time as key variables. The results showed that the gamma distribution provided the best fit compared to normal and lognormal distributions. It was also found that the recession ratio had the strongest influence on low flow quantiles, followed by dry spell characteristics. The study demonstrated that climatic and watershed properties significantly affect low flow behavior and that the proposed method can be useful in data-scarce regions.[16]

### *2.4.3 Low-Flow Seasonality and Effects on Water Availability throughout the River Network*

In this study, the effects of low-flow seasonality on water availability across a river network were investigated. The authors analyzed two common low-flow indices (Q7,10 and Q95) using both annual and monthly timescales. Results showed that annual estimates can mask significant seasonal variations, leading to inappropriate water allocation decisions. It was found that Q7,10 is generally more restrictive, while Q95 is more permissive, particularly during dry periods. Moreover, incorporating monthly variability revealed that water availability can increase in wet seasons and decrease in dry seasons. The study highlights that considering seasonality improves the accuracy of water resources management.[17]

## 2.5 Uncertainty in Climate Change Impact Studies

### *2.5.1 A framework for assessing uncertainties in climate change impacts: Low-flow scenarios for the River Thames, UK*

This study presents a probabilistic framework for assessing uncertainties associated with climate change impacts on low-flow conditions in the River Thames basin. The framework integrates multiple sources of uncertainty, including General Circulation Models (GCMs), greenhouse gas emission scenarios, downscaling techniques, and hydrological model structures and parameters. A Monte Carlo approach was applied to generate probabilistic projections of low-flow indices. The results indicate that uncertainties related to GCMs and downscaling methods have the greatest influence on projected low flows, whereas emission scenarios and hydrological model parameters play a comparatively smaller role. Additionally, variations in summer precipitation were identified as the key driver of changes in low-flow conditions. This approach provides valuable insights for risk-based water resource management under climate change.[18]

## 2.6 Ecosystem and Water Resource Perspectives

### *2.6.1 The impact of climate change on water provision under a low flow regime: A case study of the ecosystems services in the Francoli river basin*

Marqués et al. (2013) evaluated the impacts of climate change on water provisioning ecosystem services in a Mediterranean low-flow basin using the InVEST model, focusing on the Francolí River under IPCC A2 and B1 scenarios. The model estimated water yield as the difference between precipitation and evapotranspiration and assessed water availability considering land-use demand. Results showed a significant reduction in water yield (11.5–44%) mainly due to decreased precipitation. Drinking water supply declined even more (13–50%), reflecting combined effects of climate stress and demand. Spatial analysis identified northern sub-basins as the most vulnerable, with risks of severe water stress and desertification. The study also highlighted the strong influence of land use, especially in urban and agricultural areas. Overall, the results emphasize the sensitivity of water resources to climate change and the need for integrated water management.[19]

## 2.7 Conclusion

Based on the reviewed literature, the most relevant findings related to climate change impacts on low-flow conditions can be summarized as follows.

The reviewed studies can be broadly classified into three main categories:

- Studies focusing on climate change impacts on streamflow and low-flow conditions using hydrological models.
- Studies addressing low-flow characterization using statistical indices such as Q90, Q95, and drought-related metrics.
- Studies investigating uncertainties associated with climate projections, modelling approaches, and seasonal variability.

The first group of studies demonstrated that climate change significantly alters river flow regimes, particularly low-flow conditions. Most findings indicate that increasing temperature and changes in precipitation patterns lead to higher evapotranspiration and reduced water availability during dry seasons. Despite potential increases in annual precipitation, low flows tend to decrease in summer and autumn due to seasonal imbalance.

The second group of studies highlighted the importance of low-flow indices and threshold-based methods for quantifying water availability. Indices such as Q90 and Q95, as well as flow

duration curves, have been widely used to assess low-flow conditions and drought severity. These methods provide a practical framework for evaluating critical flow conditions and are particularly relevant for water resource management.

The third group of studies emphasized the role of uncertainty in climate change impact assessments. Uncertainties related to climate models, emission scenarios, and downscaling techniques were identified as major factors influencing the reliability of projections. In addition, several studies pointed out the importance of seasonal variability and basin characteristics in controlling low-flow dynamics.

Overall, the reviewed literature indicates that low-flow conditions are controlled by complex interactions between climatic factors and catchment properties, and that accurate assessment requires the integration of climate projections with hydrological modelling at the basin scale.

Based on these findings, the present study adopts a modelling framework that integrates climate projections under the RCP4.5 scenario with the SWAT hydrological model to assess low-flow conditions in the Serio River basin. Low-flow indices such as Q90 and Q95 are used to quantify changes in water availability under future climate conditions. This approach aims to provide a basin-scale assessment while addressing seasonal variability and key low-flow indicators.

# 3 Chapter 3: MATERIALS AND METHODS

## 3.1 Data Description

### *3.1.1 Observed Meteorological Data*

Daily precipitation and temperature data were obtained from ARPA Lombardia meteorological stations located within or near the Serio River basin. Four stations were selected based on spatial representativeness and data continuity:

- VALBONDIONE
- GANDELLINO – GRABIASCA
- ARDESIO – VALCANALE
- CASNIGO – CAMPO SPORTIVO

The observed dataset covers the period **2012–2025** (with station availability starting from 2004 for some stations) and includes:

- Daily precipitation (mm)
- Daily maximum and minimum air temperature (°C)

Although meteorological records were available from 2004 onward for some stations, the early portion of the dataset (2004–2007) contained a significant number of zero or missing precipitation values, likely due to measurement inconsistencies or data gaps. To ensure data reliability and avoid introducing artificial dry periods into the hydrological simulations, the effective meteorological input period for SWAT+ was defined from 2008 onward.

These observed records were used for:

- Bias correction of climate model outputs
- Reconstruction of diurnal temperature range

Observed data were downloaded directly from the ARPA Lombardia data portal.

Furthermore, Copernicus climate data used in this study are available from 2011 onward, while observed discharge (water level) data are only available from 2012. To ensure consistency and proper alignment between meteorological inputs and hydrological observations, the analysis period was therefore defined starting from 2012. This choice also guarantees temporal consistency and data reliability across all datasets and allows the selected period to be used as the baseline/reference period for subsequent analyses.

### *3.1.2 Climate Model Data*

Future climate projections were obtained from the Copernicus Climate Change Service (C3S) using the dataset “Hydrology and meteorology derived climate projections”. The dataset is

based on EURO-CORDEX regional climate model simulations with a spatial resolution of 5 km and daily temporal resolution.

The selected model configuration is summarized as follows:

- Driving GCM: ICHEC-EC-EARTH
- RCM: CLMcom-CCLM4-8-17
- Ensemble member: r12i1p1
- Spatial resolution: 5 km
- Temporal resolution: Daily
- Period: 2011–2050
- Scenario: RCP4.5
- Processing type: **Bias-corrected**

The following variables were used in this study:

- Precipitation (kg $m^{-2}$ $s^{-1}$)
- 2-m air temperature (K)

The geographic coordinates of the selected stations used for climate data extraction are presented in Table 3.1:

*Table3-1Geographic coordinates of climate stations used for data extraction*

| Station | Latitude | Longitude |
|---|---|---|
| VALBONDIONE | 46.06456797 | 10.03860694 |
| GANDELLINO | 46.00767519 | 9.94787769 |
| ARDESIO | 45.95056364 | 9.86343400 |
| CASNIGO | 45.81136488 | 9.86559107 |

### *3.1.3 Streamflow Data*

Observed daily discharge data were reconstructed from stage measurements at two gauging stations:

- Ponte Cene
- Montodine (basin outlet – Channel 1 in SWAT+)

Discharge was calculated using official stage–discharge rating curves.

For model evaluation:

- Calibration period: 2012–2020

- Validation period: 2020–2025

Observed discharge records were used to evaluate model performance using statistical efficiency metrics.

Observed discharge data for the Montodine and Ponte Cene stations were available from 2012 onward. Therefore, model calibration and performance evaluation were restricted to the period 2012–2020 (calibration) and 2020–2025 (validation), depending on data availability.

The available data consist of water level (stage height) measurements rather than direct discharge observations. Therefore, discharge values were derived using official stage–discharge rating curves provided for each station.

For the Montodine station, water level data are available from 2000 onward, while for Ponte Cene, data availability starts from 2011.

The discharge was calculated using the following piecewise equations:

Montodine:

- For $-3 \leq h \leq -0.35$ m

$$Q = 0.00027 \cdot (h + 3.9249)^{8.656}$$

- For $-0.35 \leq h \leq 1$ m

$$Q = 41.71 + 91.43h + 58.775h^2$$

Ponte Cene:

- For $0.073 \leq h \leq 0.82$ m

$$Q = 151.431 \cdot (h + 0.055)$$

- For $-0.3 \leq h \leq 0.073$ m

$$Q = 0.00022 \cdot (h + 4.445)^{7.551}$$

Using these relationships, daily discharge time series were reconstructed for both stations. These data were then used to compute mean and minimum discharge values and served as the primary reference for model calibration and low-flow analysis.

### *3.1.4 Software and Computational Environment*

The following software tools were used throughout the study:

- QGIS for spatial preprocessing
- SWAT+ Editor for watershed setup and HRU definition
- SWAT+ Toolbox for sensitivity analysis and calibration

- Python (Jupyter Notebook) for NetCDF processing and statistical analysis
- Microsoft Excel for data processing, statistical calculations, and visualization

## 3.2 SWAT+ Model Setup

### *3.2.1 Spatial Data Sources and Preparation: QGIS*

Spatial datasets required for SWAT+ model setup were obtained from pre-processed hydrological databases provided by WaterItech. These datasets include harmonized and ready-to-use layers specifically formatted for SWAT+ applications.

The following spatial datasets were used:

- Digital Elevation Model (DEM) derived from Copernicus DEM / EU-DEM
- Soil map based on the Harmonized World Soil Database (HWSD)
- Soil attribute database and lookup tables
- CORINE Land Cover 2018 dataset
- Land use lookup tables compatible with SWAT+
- River network extracted from OpenStreetMap

All spatial datasets were provided in a consistent geographic coordinate system (EPSG:4326 – WGS 84). Although the datasets were pre-processed, additional verification was performed to ensure:

- Consistent projection
- Correct spatial alignment
- Compatibility with SWAT+ input requirements
- Watershed-scale clipping after delineation

Using harmonized spatial datasets minimized preprocessing uncertainty and ensured consistency in HRU definition and watershed representation.

The watershed and HRUs were defined using the SWAT+ Editor interface.

### *3.2.2 Watershed Delineation*

The watershed was delineated using a Digital Elevation Model (Copernicus DEM / EU-DEM). Within SWAT+:

- Flow direction and accumulation were computed
- Stream network was generated
- Sub-basins were delineated
- Watershed outlet was fixed at Montodine station

The delineated basin boundary was used to clip all spatial layers.

### *3.2.3 Hydrologic Response Units (HRUs)*

HRUs were defined based on:

- Land use (CORINE Land Cover 2018)
- Soil type (HWSD database)
- Slope classification (derived from DEM)

Slope classes:

- 0–5%
- 5–15%
- 15%

Filtering method:

- Filter by landuse, soil, slope

Threshold values applied:

- Land use: 5%
- Soil: 5%
- Slope: 5%

This filtering reduced model complexity while preserving spatial heterogeneity.

### *3.2.4 Weather Input Preparation.*

#### *3.2.4.1 Observed Climate Data (ARPA)*

Observed daily precipitation and temperature data obtained from ARPA Lombardia were first quality-checked and formatted into SWAT+ text input structure.

The following files were generated:

- pcp.txt (precipitation station list file)
- tmp.txt (temperature station list file)
- Individual station files (.pcp and .tmp format) containing daily values

These files were imported into the calibrated SWAT+ project and used for historical simulation.

#### *3.2.4.2 Future Climate Data (Copernicus)*

Future climate projections were obtained in NetCDF format and processed in Python prior to model input preparation. The workflow included:

1. Extraction of station-based time series from NetCDF grids
2. Unit conversion (precipitation: kg $m^{-2}$ $s^{-1}$ to mm/day; temperature: K to °C)
3. Monthly bias correction using observed ARPA data (2011–2025 overlap period)
4. Conversion into SWAT+ weather text format
5. Generation of updated pcp.txt and tmp.txt station reference files
6. Import into the calibrated SWAT+ project for scenario simulations

### *3.2.5 Simulation Periods*

Separate simulations were conducted using:

- Observed historical forcing
- Bias-corrected Copernicus future forcing

The baseline simulation period was defined as **2012–2025**, while future simulations were conducted for the period 2026–2050.

Due to the presence of substantial missing observed discharge data prior to 2012, the baseline period was selected starting from 2012 after careful data quality assessment.

The model simulation was initiated in 2012, and the period **2012–2014** was considered as a warm-up phase to allow stabilization of soil moisture and groundwater storage. Consequently, this period was excluded from statistical analysis.

Model runs produced daily channel output files in:

channel_sd_day.txt

A total of 76 channels were generated within the watershed.

- Channel 01 → Montodine (basin outlet)
- Channel 12 → Ponte Cene (upstream station)

Daily discharge time series were extracted from these channels for calibration, validation, and low-flow analysis.

## 3.3 Model Calibration and Validation

Model calibration was conducted using SWAT+ Toolbox.

Model calibration aims to adjust model parameters within physically meaningful ranges in order to improve agreement between simulated and observed streamflow. Due to the highly

parameterized and distributed structure of SWAT+, automatic calibration was preferred over manual calibration, which is subjective and impractical for complex hydrological systems.

The calibration was performed using the **Dynamically Dimensioned Search (DDS)** algorithm implemented in the SWAT+ Toolbox. DDS is widely applied in SWAT studies because it is computationally efficient, robust, and suitable for high-dimensional parameter spaces.

Automatic calibration is generally recommended for distributed hydrological models such as SWAT, as manual calibration may introduce user bias and fail to adequately explore parameter interactions.

### *3.3.1 Calibration Strategy and Gauge Selection*

Following established hydrological practice and multi-gauge calibration studies, calibration was first conducted at the primary downstream outlet (Channel 01). Calibrating the main outlet first ensures that the integrated basin response is correctly represented before addressing upstream spatial variability.

The selection of the calibration station was based on initial model performance indicators. Since Channel 01 showed higher preliminary performance compared to Channel 12, it was considered more stable and suitable for initial parameter optimization.

### *3.3.2 Performance Evaluation Criteria*

Model performance was evaluated using the following statistical indicators:

- Nash–Sutcliffe Efficiency (NSE)
- Kling–Gupta Efficiency (KGE)
- Percent Bias (PBIAS)

Performance thresholds applied:

- NSE > 0.5 → Acceptable
- NSE > 0.75 → Very Good
- KGE between 0.5–0.7 → Good
- KGE ≈ 1 → Excellent

KGE was selected as the primary objective function because it simultaneously evaluates:

1. Correlation (temporal dynamics)
2. Bias (mean flow deviation)
3. Variability (flow dispersion)

The conceptual formulation of KGE is:

$$KGE = 1 - \sqrt{(r-1)^2 + (\beta-1)^2 + (\gamma-1)^2}$$

Compared to NSE, KGE provides a more balanced assessment of daily discharge simulations, particularly for low-flow studies.

As shown in Figure 3.1, the model is able to reasonably reproduce the observed streamflow dynamics during the calibration period.


*Figure 3.1Observed and simulated daily streamflow during the calibration period*

### *3.3.3 Sensitivity Analysis*

Prior to calibration, a global sensitivity analysis was conducted using Sobol first-order indices to identify the most influential parameters controlling streamflow.

Given the large number of parameters in SWAT, calibrating all parameters is neither computationally efficient nor scientifically justified. Sensitivity analysis allows identification of dominant parameters and reduces equifinality.

Figure 3.2 illustrates the selected sensitive parameters and their defined variation ranges used in the calibration process.

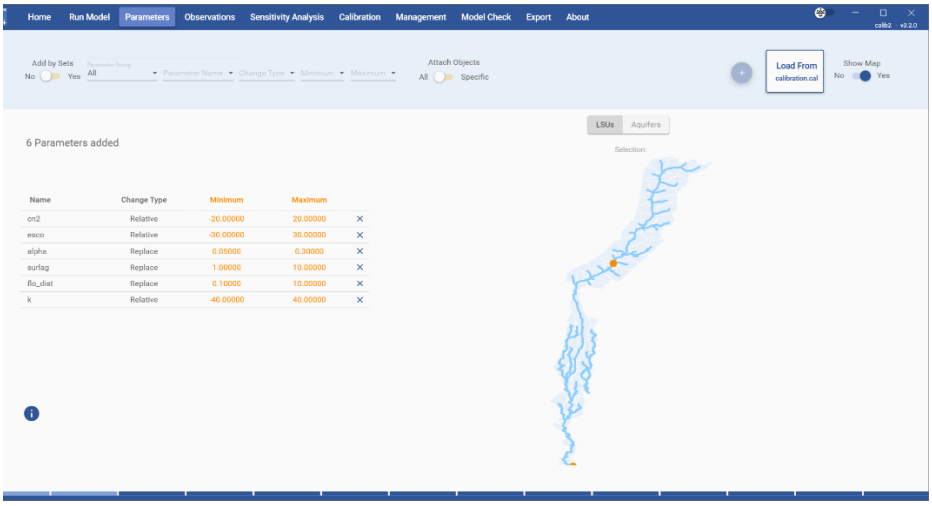


*Figure 3.2Selected sensitive parameters and their variation ranges used for model calibration*

The most sensitive parameters identified based on Sobol first-order indices are summarized in Table 3.2.

*Table3-2Most sensitive parameters identified using Sobol first-order sensitivity analysis*

| **Parameter** | **Group** |
|---|---|
| SOL_K | Soil |
| SURLAG | Basin |
| ESCO | HRU |
| CN2 | HRU |
| ALPHA | Aquifer |
| FLO_DIST | Aquifer |

Values greater than 0.1 indicate significant influence on discharge response, while values close to zero or negative suggest negligible contribution under current model conditions.

### *3.3.4 Parameter Selection for Calibration*

Based on sensitivity results, only the two most influential parameters were retained for calibration:

- SOL_K (Relative change: −50% to +50%)
- SURLAG (Replace: 1–10 days)

Non-sensitive parameters (CN2, ESCO, ALPHA, FLO_DIST) were excluded to avoid unnecessary model instability and parameter interaction.

Restricting calibration to sensitive parameters improves model identifiability and reduces equifinality.

### *3.3.5 Calibration Period (2012–2020)*

The calibration period was defined from 2012 to 2020, including a two-year warm-up period to minimize the influence of initial conditions on model response. The warm-up period allows soil moisture and groundwater storage components to stabilize before performance evaluation. Calibration was conducted using the DDS algorithm, focusing exclusively on the most sensitive parameters identified in the Sobol analysis (SOL_K and SURLAG). Parameter ranges were defined within physically meaningful limits to ensure hydrological realism.

Model performance was evaluated using multiple complementary statistical indicators:

Nash–Sutcliffe Efficiency (NSE) – measures goodness-of-fit relative to observed variance

Kling–Gupta Efficiency (KGE) – evaluates correlation, bias, and variability simultaneously

Percent Bias (PBIAS) – indicates systematic over- or underestimation

Among these, KGE was adopted as the primary objective function, as it provides a more balanced evaluation of daily discharge performance, particularly relevant for low-flow analysis.

### *3.3.6 Validation Period (2023–2025)*

The validation period was defined from 2023 to 2025. The calibrated parameter set obtained during the calibration phase was applied without any further modification.

Validation serves as an independent test of model robustness under unseen conditions. Maintaining parameter values unchanged ensures that model predictive capability is evaluated objectively.

The model maintained reasonable correlation structure and bias control, suggesting that the parameterization is physically meaningful rather than overfitted to the calibration period.

## 3.4 Climate Data Processing

### *3.4.1 NetCDF Processing in Python*

NetCDF climate datasets were processed in a Python-based computational environment to extract station-level time series compatible with SWAT+.

Initial inspection of the NetCDF datasets was carried out using Python libraries (xarray). Data extraction and preprocessing were carried out in Jupyter Notebook using the Python libraries xarray, dask, pandas, and NumPy.

The workflow included:

- Loading large NetCDF datasets using lazy loading (xarray with dask)
- Identification of grid cells corresponding to meteorological station coordinates using nearest-neighbor selection
- Unit conversion of precipitation from kg $m^{-2}$ $s^{-1}$ to mm/day using:

$$P(mm/day) = prAdjust \times 86400$$

- Export of extracted time series into CSV format
- Temporal alignment with observed datasets
- Verification of continuity and missing values

This workflow reduced dataset size significantly and produced station-based climate time series suitable for bias correction and SWAT+ meteorological input preparation.

### *3.4.2 Climate Bias Correction*

Although the Copernicus dataset is provided as bias-adjusted at the European scale, an independent verification was performed to assess whether residual local bias remained at the watershed scale.

To ensure local reliability, the historical Copernicus climate data (2011–2025) corresponding to the RCP 4.5 scenario were extracted at the exact coordinates of the selected meteorological stations and directly compared with observed daily precipitation and temperature records obtained from ARPA Lombardia for the same period.

Days with missing values in observed datasets were excluded from the statistical comparison to ensure consistent pairing.

The comparison was conducted at both daily and monthly scales.

Results showed:

Systematic underestimation of precipitation

Seasonal temperature offsets

Reduced representation of local extremes

These discrepancies confirm that continental-scale bias adjustment does not guarantee removal of local systematic errors, particularly in mountainous basins.

Therefore, an additional **station-based bias correction procedure** was applied using observed data as reference.

#### *3.4.2.1 Temperature Bias Correction Using the Monthly Additive Delta Method*

The objective of this method is to remove systematic temperature bias while preserving the projected climate change signal, particularly the long-term warming trend.

A reference period of 2012–2025 was selected, corresponding to the common overlap between observed temperature data from ARPA Lombardia and historical Copernicus climate data.

For each meteorological station, daily temperature values were grouped by calendar month (January to December) over the entire reference period. Monthly mean temperatures were then calculated separately for observed data and model outputs. This resulted in 12 observed and 12 modeled monthly mean temperature values for each station.

The monthly bias (Δ) was computed as the difference between observed and modeled mean temperatures. Positive values indicate underestimation by the model, while negative values indicate overestimation. This procedure produced a set of 12 monthly correction factors.

These correction values were subsequently applied to future daily temperature data. For each day, the corresponding monthly correction was added to the raw Copernicus temperature value. The additive delta method is appropriate for temperature correction, as temperature bias typically manifests as a systematic offset. This approach preserves daily variability and long-term trends while correcting the mean bias. It also assumes that the monthly bias structure remains stationary over time.

#### *3.4.2.2 Precipitation Bias Correction Using Monthly Multiplicative Scaling*

The purpose of this method is to correct systematic biases in precipitation while preserving the relative changes projected by the climate model.

The same reference period (2012–2025) was used. For each station and each calendar month, daily precipitation values were grouped and monthly mean precipitation was calculated for both observed and modeled datasets.

A multiplicative bias correction factor was then computed as the ratio of observed to modeled monthly mean precipitation. Values greater than one indicate underestimation by the model, while values less than one indicate overestimation. This resulted in 12 monthly correction factors for each station.

These factors were applied to future daily precipitation values by multiplying each modeled value by the corresponding monthly factor. If the modeled precipitation was zero, the corrected value remained zero.

Unlike temperature, precipitation bias is generally proportional rather than additive. Therefore, multiplicative scaling is more appropriate, as it preserves the structure of wet and dry days, maintains relative intensity, and retains the projected climate change signal.

**Important Assumption:**

Both correction methods rely on the assumption that bias characteristics remain stationary over time, meaning that the monthly bias structure identified during the reference period is representative of future conditions. This assumption is commonly adopted in hydrological climate impact studies.

### *3.4.3 Reconstruction of Tmin and Tmax*

The Copernicus climate dataset used in this study provides only daily mean air temperature (tasAdjust), whereas the SWAT+ model requires daily minimum (Tmin) and maximum (Tmax) temperature as mandatory inputs. To address this limitation, a reconstruction procedure was implemented to derive Tmin and Tmax from the available mean temperature data.

SWAT+ relies on daily temperature range for the simulation of several key processes, including potential evapotranspiration, plant growth, and soil temperature dynamics. Therefore, the absence of Tmin and Tmax in the input dataset necessitated a physically consistent method to reconstruct these variables.

The reconstruction approach is based on the assumption that the diurnal temperature range (DTR), defined as the difference between daily maximum and minimum temperature, remains relatively stable at the monthly scale between historical and future periods.

Using observed ARPA temperature data for the reference period 2012–2025, the daily temperature range was first calculated for each day as the difference between observed Tmax and Tmin. These daily values were then grouped by calendar month, and the mean monthly diurnal temperature range was computed for each station. This resulted in a set of 12 representative monthly DTR values.

The derived monthly DTR values were then used to reconstruct Tmin and Tmax from the Copernicus daily mean temperature. For each day, Tmin was estimated by subtracting half of the corresponding monthly DTR from the daily mean temperature, while Tmax was obtained by adding the same amount. In this way, the reconstructed temperature series preserves the original mean temperature signal while introducing a realistic daily range.

This method assumes that the seasonal pattern of the diurnal temperature range does not change significantly over time and that climate change primarily affects mean temperature rather than

intra-daily variability. Such assumptions are commonly adopted in hydrological climate impact studies when only mean temperature projections are available.

The applied reconstruction approach ensures consistency with SWAT+ input requirements, maintains realistic seasonal variability, and preserves the projected warming signal. Without this step, the use of future climate data within the SWAT+ framework would not be feasible.

## 3.5 Future Scenario Simulation

Future climate impact simulations were performed using the same calibrated SWAT+ model **configuration** developed during the historical calibration phase. No structural modifications were made to the model after calibration.

The optimized parameter set obtained from the calibration period was retained unchanged and directly transferred to the future simulations to ensure consistency and to isolate the effect of climate forcing on hydrological response.

Bias-corrected daily precipitation and temperature projections obtained from the Copernicus Climate Data Store (EURO-CORDEX, RCP4.5) were prepared in SWAT+ weather input format and imported into the calibrated SWAT+ project. Only the meteorological forcing data were replaced, while all watershed, soil, land use, routing, and calibrated hydrological parameters remained identical to the validated historical setup.

The model was then executed for the period 2026–2050 under the RCP4.5 scenario. The resulting daily discharge outputs were extracted from the channel output file (channel_sd_day.txt) for subsequent low-flow and hydrological drought analysis.

This approach ensures that any differences between baseline and future discharge conditions are attributable solely to projected climate changes rather than alterations in model structure or parameterization.

## 3.6 Low-Flow Analysis

Low-flow conditions were evaluated using the Q95 indicator, defined as the discharge exceeded 95% of the time and widely used to characterize hydrological drought conditions. The analysis was applied to simulated discharge obtained from the calibrated SWAT+ model for the baseline period and to simulated discharge under future climate conditions.

Prior to the analysis, the discharge time series were checked for temporal continuity to ensure reliable comparison between baseline and future simulations.

Low-flow conditions for the baseline period were derived from model-simulated discharge rather than directly from observed data. This approach ensures methodological consistency, as both baseline and future low-flow indicators are based on the same modeling framework. In addition, using simulated discharge allows the effect of climate forcing to be isolated while avoiding inconsistencies related to observational limitations and data gaps.

The Q95 values were computed from daily discharge time series for each simulation period and applied consistently to both baseline and future conditions. This unified approach enables a direct and robust comparison of changes in low-flow magnitude under projected climate scenarios.

# 4 Chapter 4: RESULTS

## 4.1 Basin Characteristics and Model Configuration Output

The delineation of the Serio River basin was performed using a Digital Elevation Model (DEM) within the SWAT+ modeling environment. This process resulted in the generation of the river network, sub-basins, and Hydrological Response Units (HRUs), which together define the spatial framework used by the model to simulate hydrological processes.

As illustrated in Figure 4.1, the SWAT+ model delineates the Serio River basin and represents the river network and sub-basin structure of the study area.

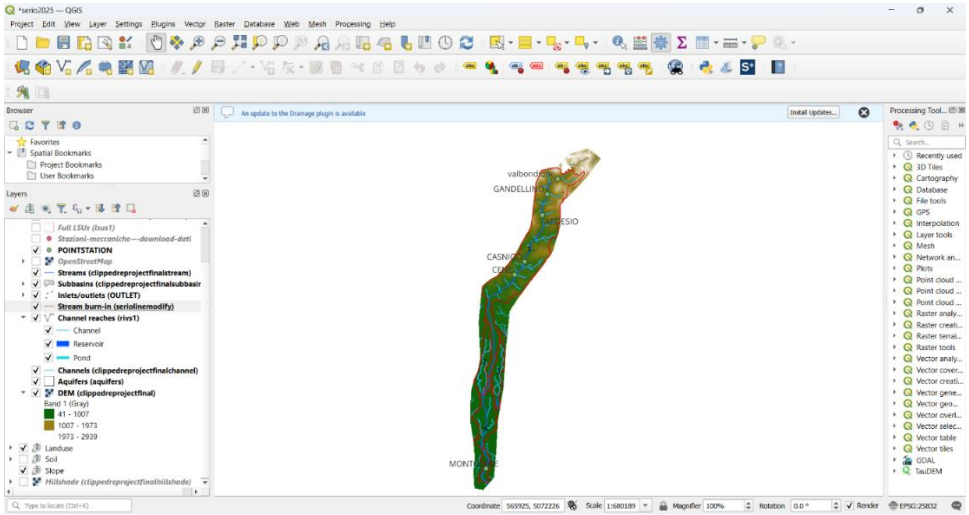

*Figure 4.1 Delineated Serio River basin and river network generated in SWAT+*

The total modeled watershed area is 58,331.15 hectares (approximately 583.3 km²). The basin was divided into four sub-basins, representing the main drainage structure of the catchment.

Within these sub-basins, a total of 241 Hydrological Response Units (HRUs) were generated. HRUs represent unique combinations of land use, soil type, and slope, allowing the model to capture the spatial heterogeneity of the basin.

The extracted drainage network consists of 76 channels, which define the routing pathways for water flow through the basin. These channels connect different landscape units and control the downstream transport of water and sediments.

In addition, the model configuration includes six aquifers, representing groundwater storage components that contribute to baseflow generation and help sustain streamflow during dry periods.

Furthermore, 76 routing units and 76 landscape units were defined within the model to simulate key hydrological processes, including runoff generation, infiltration, evapotranspiration, and groundwater flow.

The main spatial characteristics of the SWAT+ model setup for the Serio River basin are summarized in Table 4.1.

*Table4-1Summary of SWAT+ spatial model configuration for the Serio River basin*

| Parameter | Value |
|---|---|
| **Total basin area** | **58,331.15 ha (≈583.3 km²)** |
| **Number of subbasins** | **4** |
| **Number of HRUs** | **241** |
| **Number of channels** | **76** |
| **Number of aquifers** | **6** |
| **Routing units** | **76** |
| **Landscape units** | **76** |
| **Reservoirs** | **0** |

Overall, the spatial discretization of the basin allows the SWAT+ model to effectively represent variations in topography, land use, and soil properties. This configuration provides the structural basis for the hydrological simulations and the climate change impact analysis presented in the following sections.

## 4.2 SWAT Model Performance

### *4.2.1 Sensitivity Analysis and Calibration Parameters*

Sobol first-order sensitivity analysis revealed that discharge variability was primarily controlled by:

- SOL_K (Soil hydraulic conductivity) – 0.6086 (Highly sensitive)
- SURLAG (Surface runoff lag time) – 0.3092 (Sensitive)

Other parameters (ESCO, CN2, ALPHA, FLO_DIST) were negligible and excluded to reduce equifinality.

Calibration was therefore restricted to SOL_K and SURLAG.

Optimal Parameter Set (Channel 01)

- SOL_K = −22.13% (relative change)
- SURLAG = 1 day

This indicates reduced effective infiltration and rapid catchment response.

Effect of Calibration on Model Performance:

To evaluate the effectiveness of calibration, simulated discharge before and after parameter optimization was directly compared with observed discharge at Channel 01 (primary outlet) and Channel 12 (secondary station).

### *4.2.2 Pre-Calibration vs Post-Calibration Performance*

- **Channel 01 (Montodine)**

Model performance at the main outlet (Channel 01 – Montodine) before and after calibration is presented in Table 4.2.

*Table4-2Model performance at Channel 01 (Montodine) before and after calibration*

| Metric | Before Calibration | After Calibration | Change |
|---|---|---|---|
| KGE | 0.65 | 0.75 | ↑ +0.10 |
| NSE | 0.30 | 0.56 | ↑ +0.26 |
| PBIAS | 11.61% | 11.34% | Slight reduction |

At this Channel, calibration resulted in a clear improvement in model performance.

- KGE increased from 0.65 to 0.75, indicating stronger agreement in correlation, variability, and bias.
- NSE increased from 0.30 to 0.56, demonstrating improved reproduction of daily discharge dynamics.
- PBIAS slightly decreased, indicating more stable representation of flow magnitude.

These improvements confirm that the calibration significantly enhanced the model's ability to reproduce observed discharge at the basin outlet.

Model performance at Channel 12, using parameters calibrated at Channel 01, is presented in Table 4.3.

*Table4-3Model performance at Channel 12*

| Metric | Before Calibration | After Calibration | Change |
|---|---|---|---|
| KGE | 0.27 | 0.39 | ↑ +0.12 |

| Metric | Before Calibration | After Calibration | Change |
|---|---|---|---|
| NSE | −0.59 | −0.14 | Improved but still weak |
| PBIAS | 60.28% | 53.64% | ↓ Reduced bias |

At Channel 12, the application of parameters calibrated at Channel 01 resulted in noticeable, although limited, improvements in model performance.

KGE increased from 0.27 to 0.39, indicating some improvement in the agreement between observed and simulated discharge. NSE also improved from −0.59 to −0.14, suggesting a better representation of discharge dynamics, although the values remain unsatisfactory.

PBIAS decreased from 60.28% to 53.64%, reflecting a reduction in bias, yet still indicating a substantial overestimation or underestimation of flow magnitude.

Overall, these results suggest that basin-scale calibration can partially improve model performance at upstream locations; however, local hydrological variability is not fully captured.

### *4.2.3 Validation Period (2020–2025)*

**Channel 01 (Validation)**

Model performance at Channel 01 during the calibration and validation periods is presented in Table 4.4.

*Table4-4Model performance at Channel 01 during calibration and validation periods*

| Metric | Calibration Period | Validation Period |
|---|---|---|
| KGE | 0.75 | 0.63 |
| NSE | 0.56 | 0.51 |
| PBIAS | 11.34% | 27.46% |

Calibration results indicate that the model maintains an acceptable level of performance during the validation period.

KGE decreased slightly from 0.75 to 0.63, while NSE declined from 0.56 to 0.51, indicating a minor reduction in model accuracy. PBIAS increased from 11.34% to 27.46%, suggesting a higher deviation in simulated discharge magnitude during validation.

Overall, despite this expected reduction in performance, the model retains a reasonable predictive capability, confirming its robustness.

- **Channel 12 (Validation)**

Model performance at Channel 12 during calibration and validation periods is presented in Table 4.5.

*Table4-5Model performance at Channel 12 during calibration and validation periods*

| Metric | After Calibration | Validation |
|---|---|---|
| KGE | 0.39 | 0.49 |
| NSE | −0.14 | 0.14 |
| PBIAS | 53.64% | 46.05% |

At Channel 12, validation results indicate a moderate improvement compared to the calibration phase.

KGE increased from 0.39 to 0.49, and NSE improved from −0.14 to 0.14, suggesting a better representation of discharge dynamics. Additionally, PBIAS decreased from 53.64% to 46.05%, indicating a reduction in bias.

However, despite these improvements, model performance at Channel 12 remains weaker than at the basin outlet, highlighting the challenges in capturing local hydrological variability.

### *4.2.4 Additional Calibration Attempt at Channel 12*

A separate sensitivity analysis confirmed SOL_K and SURLAG as dominant parameters.

Optimized values:

- SURLAG = 1
- SOL_K = −30.26%

However, the resulting model performance did not show improvement and returned to values similar to the pre-calibration condition.

As shown in Table 4.6, KGE remained low (0.27), NSE was negative (−0.59), and PBIAS remained high (60.28%), indicating poor model performance.

*Table4-6Model performance at Channel 12 after independent calibration*

| Metric | Result |
|---|---|
| KGE | 0.27 |
| NSE | −0.59 |
| PBIAS | 60.28% |

This indicates that independent calibration at Channel 12 did not produce stable improvement, reinforcing that Channel 01 is the most reliable basin-scale calibration point.

### *4.2.5 Comparative Analysis of Model Performance After Calibration*

Following the completion of the calibration process, an additional comparison was conducted to evaluate the overall model performance. This analysis focuses on the comparison between observed and simulated discharge under pre- and post-calibration conditions.

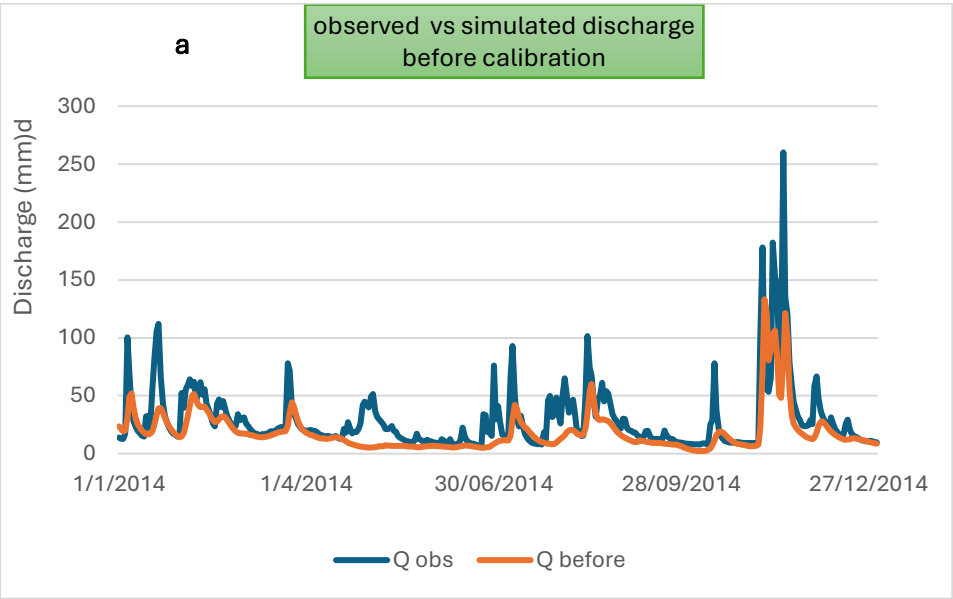


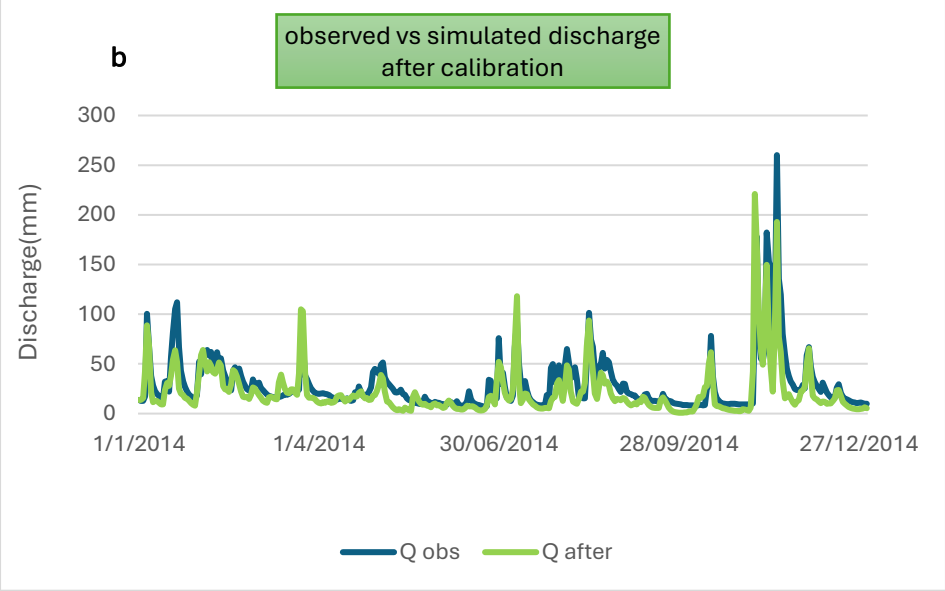

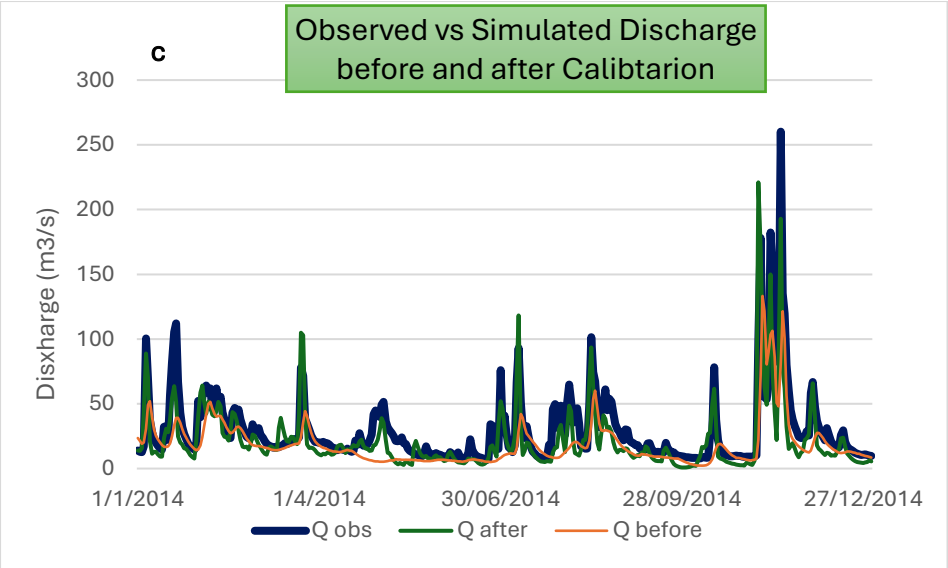


*Figura 4.2 Observed and simulated discharge at Channel 1 ( montodine) under different conditions: (a) pre-calibration, (b) post-calibration, and (c) comparison of observed, pre- and post-calibration simulations.*

Figures 4.2 (a–c) illustrate the comparison between observed and simulated discharge before and after calibration at Channel 01 (Montodine).

The results show that the calibrated simulation follows the observed hydrograph more closely than the pre-calibration simulation. Improvements are particularly evident in peak flow magnitude and low-flow representation.

Overall, calibration improved model performance, as reflected by increased agreement with observed discharge and a better representation of flow variability.

## 4.3 Climate Bias Assessment Results

Although the Copernicus dataset is labeled as bias-adjusted at the European scale, an independent evaluation was conducted to assess the presence of residual local-scale bias within the Serio River basin.

Copernicus historical climate data under the RCP 4.5 scenario (2011–2025) were extracted and compared against observed meteorological records obtained from ARPA Lombardia for the same period. The comparison was performed at both daily and monthly temporal scales.

Prior to statistical evaluation, data cleaning was performed. Days with missing values in either observed or simulated datasets were excluded to avoid artificial distortion of performance metrics.

### *4.3.1 Pre-Correction Climate Comparison*

#### *4.3.1.1 Precipitation*

Comparison between ARPA observations and Copernicus precipitation over the reference period (2011–2025) reveals substantial systematic discrepancies.
Daily and monthly precipitation statistics are summarized in Table 4.7.

*Table4-7Statistical comparison between ARPA observations and Copernicus precipitation (2011–2025)*

| **Station** | **PBIAS (%)** | **Daily RMSE (mm)** | **Daily Corr** | **Monthly RMSE (mm)** | **Monthly Corr** |
|---|---|---|---|---|---|
| Valbondione | -31.55 | 16.72 | 0.028 | 141.71 | 0.193 |
| Gandellino | -27.61 | 15.13 | 0.039 | 122.39 | 0.220 |
| Ardesio | -41.98 | 20.04 | 0.038 | 176.45 | 0.195 |
| Casnigo | -27.00 | 12.93 | 0.020 | 108.29 | 0.167 |

**Interpretation**
The results indicate a systematic underestimation of precipitation across all stations, with PBIAS values ranging between −27% and −42%.
The extremely low daily correlation coefficients (**0.02–0.04**) suggest that Copernicus data are not able to accurately reproduce the timing of daily precipitation events at the basin scale. Although the correlation slightly improves at the monthly scale (**≈0.17–0.22**), it remains relatively weak, indicating the persistence of structural bias.
Furthermore, the monthly RMSE values (**108–176 mm**) highlight substantial deviations in accumulated precipitation.
As shown in Figure 4.7, Copernicus precipitation consistently underestimates observed values across all stations, particularly during peak rainfall months. This pattern is evident at Gandelino, Casnigo, Ardesio, and Valbondione, where the differences between observed and simulated precipitation are more pronounced during high-precipitation periods.
Overall, these findings confirm that continental-scale bias correction does not fully eliminate local-scale systematic errors, particularly in mountainous catchments such as the Serio River basin.

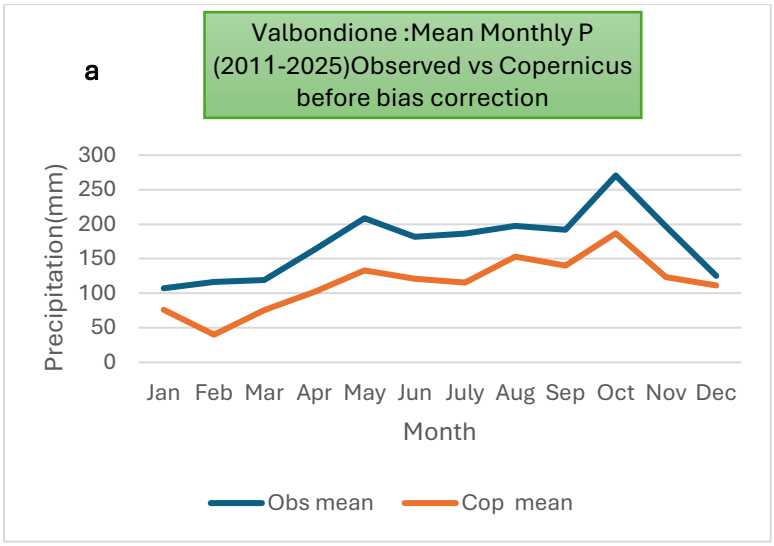
a
Valbondione :Mean Monthly P (2011-2025)Observed vs Copernicus before bias correction
Precipitation(mm)
300
250
200
150
100
50
0
Jan Feb Mar Apr May Jun July Aug Sep Oct Nov Dec
Month
Obs mean
Cop mean

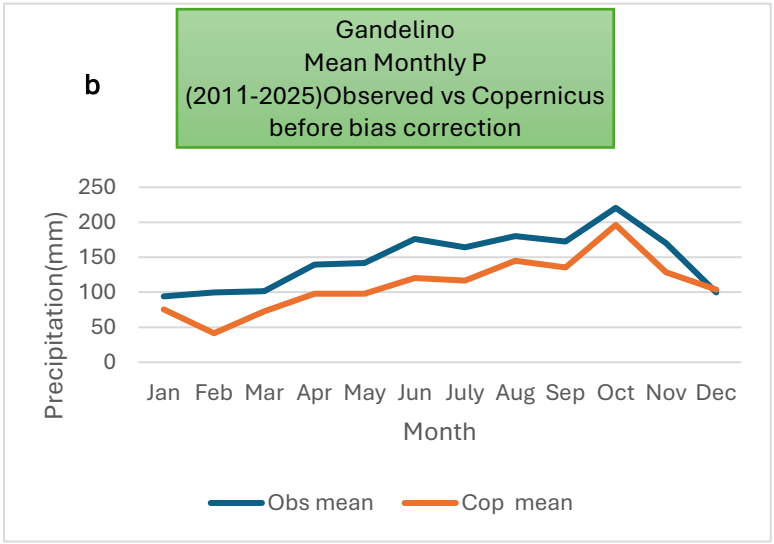
b
Gandelino
Mean Monthly P
(2011-2025)Observed vs Copernicus before bias correction
Precipitation(mm)
250
200
150
100
50
0
Jan Feb Mar Apr May Jun July Aug Sep Oct Nov Dec
Month
Obs mean
Cop mean

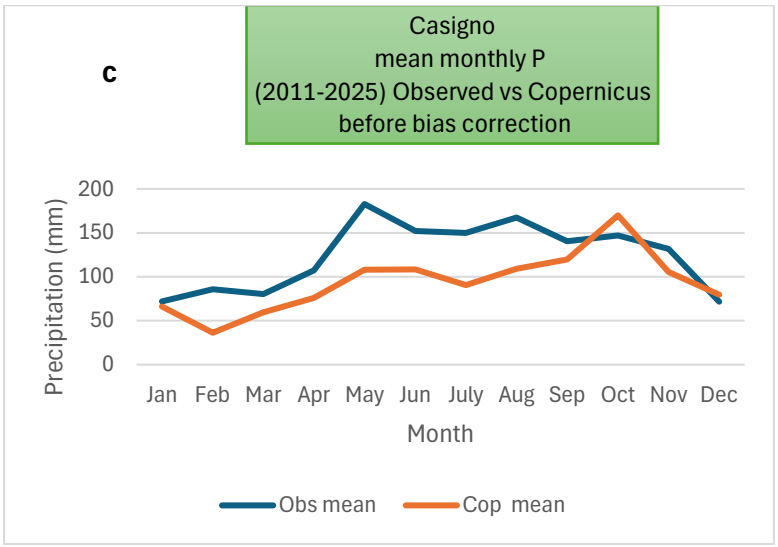
c
Casigno
mean monthly P
(2011-2025) Observed vs Copernicus before bias correction
Precipitation (mm)
200
150
100
50
0
Jan Feb Mar Apr May Jun July Aug Sep Oct Nov Dec
Month
Obs mean
Cop mean

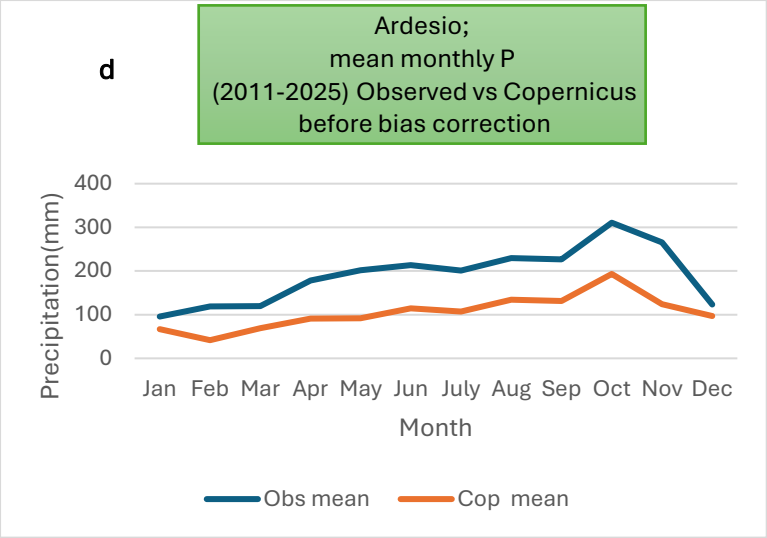


*Figura 4.3Observed and Copernicus mean monthly precipitation (2011–2025) before bias correction at four stations: (a) Valbondione, (b) Gandelino, (c) Casnigo and (d) Ardesio*

#### *4.3.1.2 Temperature*

Temperature comparison revealed smaller, yet still systematic, deviations between Copernicus data and ARPA observations.

Daily mean temperature from Copernicus was compared against ARPA observations over the reference period (2011–2025). The statistical results at both daily and monthly scales are summarized in Table 4.8.

*Table4-8 Statistical comparison of observed and Copernicus temperature (2011–2025)*

| **Station** | **PBIAS (%)** | **Daily RMSE (°C)** | **Daily Correlation** | **Monthly RMSE (°C)** | **Monthly Correlation** |
|---|---|---|---|---|---|
| Valbondione | -39.505 | 5.316 | 0.763 | 3.552 | 0.925 |
| Gandelino | -50.57 | 6.629 | 0.843 | 5.667 | 0.955 |
| Ardesio | -34.992 | 5.401 | 0.837 | 4.044 | 0.952 |
| Casnigo | -16.399 | 4.358 | 0.873 | 2.866 | 0.963 |

Interpretation

In contrast to precipitation, both daily and monthly correlations are high (>0.75 at the daily scale and >0.90 at the monthly scale), indicating that Copernicus data are able to accurately reproduce the temporal variability of temperature.

However, a systematic negative bias is observed in the mean values, suggesting a consistent underestimation of temperature magnitude.

This indicates that the primary source of error in temperature data is related to a bias in the mean values rather than inaccuracies in variability or temporal dynamics.

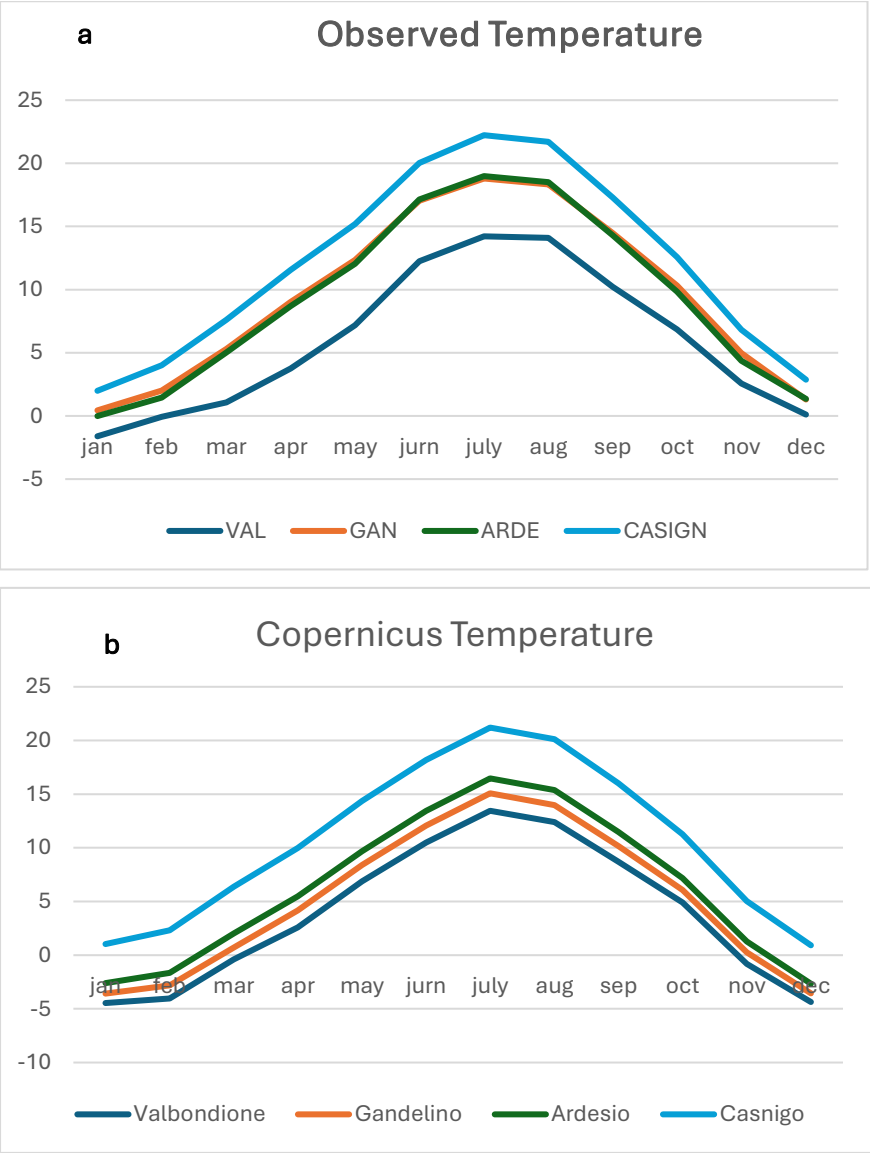


*Figura 4.4Mean monthly temperature (2011–2025) at four stations: comparison between (a) observed data and (b) Copernicus data.*

As shown in Figure 4.4, Copernicus temperature closely follows the observed seasonal pattern at all stations, with only minor deviations in magnitude**.**

### *4.3.2 Magnitude of Bias Factors*

Based on the analysis of the reference period, monthly bias correction factors were derived for both precipitation and temperature at each station.

Precipitation correction factors exhibit strong seasonal variability, with larger scaling factors during winter months and relatively smaller factors during summer. This pattern reflects stronger underestimation of winter precipitation by the climate model.

Temperature delta values also show seasonal structure, with larger corrections required during colder months.

Overall, precipitation bias magnitude is considerably larger than temperature bias in relative terms, confirming that precipitation constitutes the dominant source of climatic uncertainty in the basin.

Detailed monthly bias correction factors are provided in Appendix A (Tables A.1 and A.2).

### *4.3.3 Implications for Hydrological Modeling*

The identified systematic underestimation in precipitation and temperature magnitude would directly affect hydrological simulations if uncorrected.

In particular:

- Underestimated precipitation would lead to reduced simulated runoff and low-flow overestimation.
- Negative temperature bias would affect evapotranspiration and seasonal flow dynamics.

Therefore, the quantified monthly bias factors were subsequently applied to future

## 4.4 Projected Climate Change Signal (2027–2050 vs 2014–2025)

This section presents the projected changes in temperature and precipitation under future climate conditions relative to the baseline period (2014–2025). All values are derived from bias-corrected climate projections.

### *4.4.1 Projected Temperature Changes*

Mean annual and seasonal temperature differences between the baseline (2014–2025) and future period (2027–2050) were computed.

Detailed values are provided in Appendix B.

The comparison between the baseline period (2014–2025) and the future climate period (2027–2050) indicates a consistent warming signal across all meteorological stations in the Serio River basin.

At Valbondione, the mean annual temperature increases from 5.99°C to 6.41°C, corresponding to a warming of +0.42°C. Seasonal analysis shows that the strongest warming occurs during spring (+0.60°C) and autumn (+0.56°C), while winter temperature increases are relatively small (+0.06°C).

At Gandellino, the annual mean temperature increases from 9.73°C to 10.10°C, representing a warming of +0.37°C. Temperature increases are observed in all seasons, with the largest changes occurring during winter (+0.59°C) and autumn (+0.59°C).

At Ardesio, mean annual temperature increases from 9.51°C to 9.85°C (+0.34°C). Seasonal changes show moderate warming during spring (+0.47°C), summer (+0.63°C), and autumn (+0.56°C), while winter temperatures show a negligible decrease (−0.11°C).

At Casnigo, the annual temperature increases from 12.27°C to 12.48°C, corresponding to a warming of +0.21°C. The strongest warming occurs during summer (+0.54°C) and autumn (+0.47°C), whereas winter temperatures slightly decrease (−0.28°C).

Overall, the results indicate a general warming trend across the basin, with annual temperature increases ranging from approximately +0.21°C to +0.42°C depending on station location. Seasonal analysis shows that summer and autumn exhibit the most consistent warming signals, while winter changes remain relatively small and locally variable.

This warming pattern may have important hydrological implications, particularly through increased evapotranspiration during the warm season, which could contribute to enhanced low-flow conditions in the basin.

### *4.4.2 Projected Precipitation Changes*

Projected precipitation totals were compared between the baseline (2014–2025) and future period (2027–2050).

Detailed values are provided in Appendix C.

The comparison between the baseline period (2014–2025) and the future climate period (2027–2050) indicates a general decrease in annual precipitation across all meteorological stations in the basin, although the magnitude and seasonal distribution of changes vary spatially.

At Valbondione, mean annual precipitation decreases from 5.73 mm to 5.52 mm, corresponding to a reduction of approximately −3.66%. Seasonal analysis indicates a pronounced decrease

during winter (−16.23%) and autumn (−13.05%), while spring precipitation increases by about +9.39%. Summer precipitation shows only minor changes.

At Gandellino, annual precipitation decreases slightly from 4.87 mm to 4.70 mm (−3.88%). The most significant reductions occur during autumn (−16.23%) and winter (−12.82%), whereas spring precipitation increases by nearly +9.78%, and summer precipitation remains nearly unchanged.

At Ardesio, annual precipitation decreases more substantially, from 6.64 mm to 6.02 mm, corresponding to a reduction of −8.93%. The largest seasonal decrease occurs during autumn (−30.59%), indicating a considerable reduction in precipitation during this period. Summer precipitation slightly increases (+2.92%), while winter and spring changes remain relatively small.

At Casnigo, annual precipitation decreases from 4.08 mm to 3.68 mm (−9.58%), representing the strongest annual reduction among the four stations. Seasonal analysis reveals a significant decrease during autumn (−22.4%) and summer (−13.20%), while spring precipitation shows a small increase (+2.67%).

Overall, the results indicate a general reduction in annual precipitation across the basin, with decreases ranging from approximately −3.7% to −9.6% depending on station location. Seasonal patterns reveal a consistent reduction in autumn precipitation across all stations, while spring precipitation tends to increase slightly. Summer precipitation changes are relatively small and spatially variable.

These seasonal shifts in precipitation distribution may have important hydrological implications. In particular, the reduction in autumn and winter precipitation, combined with projected temperature increases during the warm season, may contribute to increased evapotranspiration and reduced water availability, potentially intensifying low-flow conditions in the Serio River basin.

## 4.5 Future Hydrological Response

To evaluate the hydrological response of the Serio River basin to projected climate changes, river discharge during the future period (2027–2050) simulated by the calibrated SWAT+ model was compared with observed discharge data obtained from the ARPA monitoring network for the baseline period (2014–2025).

Mean discharge values were calculated at both annual and seasonal scales for the two hydrological stations located along the Serio River: Cene and Montodine.

Detailed discharge values are provided in Appendix D.

The comparison between observed baseline discharge and future simulated discharge indicates a substantial reduction in river flow under projected climate conditions.

At the Cene station, the results show a pronounced decline in discharge across all seasons. Mean annual discharge decreases from 19.77 m³/s during the baseline period to 5.40 m³/s under future conditions, corresponding to a reduction of approximately −72.7%. Seasonal analysis reveals consistent reductions throughout the year, including −65.6% in winter, −77.0% in spring, −76.3% in summer, and −69.5% in autumn. These results indicate a strong reduction in water availability in the upstream part of the basin.

At the Montodine station, the projected reductions are less pronounced but still clearly observable. Mean annual discharge decreases from 17.11 m³/s in the baseline period to 12.61 m³/s in the future period, corresponding to a decline of approximately −26.3%. Seasonal analysis indicates moderate reductions during winter (−15.3%), spring (−15.8%), summer (−35.2%), and autumn (−36.8%).

Overall, the results indicate that projected climate changes may significantly alter both the magnitude and seasonal distribution of river discharge within the Serio River basin. The strongest reductions occur during the summer season, which represents a critical period for water availability.

These changes are consistent with the previously identified climate signals, including increasing air temperature and reductions in precipitation, which together may enhance evapotranspiration and reduce effective runoff. Furthermore, the larger reductions observed at the Cene station compared to Montodine suggest that upstream sections of the basin may be more sensitive to projected climate changes.

## 4.6 Low-Flow Analysis

### *4.6.1 Monthly Low-Flow Analysis*

It should be noted that, unlike the comparison presented in Section 4.5, low-flow indicators (Q95) were derived from SWAT-simulated discharge for both baseline and future periods. This approach ensures methodological consistency, as percentile-based low-flow metrics are sensitive to distributional properties and require a consistent modeling framework for reliable comparison.

The monthly variation of Q95 values was analyzed to assess the seasonal response of low-flow conditions under baseline (2014–2025) and future (2026–2050) climate scenarios.

*Table4-9Monthly Q95 values under baseline (2014–2025) and future (2026–2050) conditions at Cene and Montodine stations*

| Month | Cene Baseline | Cene Future | Change (%) | Montodine Baseline | Montodine Future | Change (%) |
|---|---|---|---|---|---|---|
| Jan | 0.154 | 0.656 | +325% | 0.639 | 2.374 | +271% |
| Feb | 0.182 | 0.580 | +219% | 0.699 | 2.024 | +190% |
| Mar | 0.182 | 0.630 | +246% | 1.177 | 1.932 | +64% |
| Apr | 0.871 | 0.468 | −46% | 2.289 | 1.727 | −25% |
| May | 1.937 | 0.500 | −74% | 6.554 | 1.346 | −79% |
| Jun | 0.942 | 0.411 | −56% | 1.813 | 1.039 | −43% |
| Jul | 0.507 | 0.226 | −55% | 0.825 | 0.517 | −37% |
| Aug | 0.833 | 0.092 | −89% | 2.442 | 0.007 | −99% ❗ |
| Sep | 0.812 | 0.096 | −88% | 3.038 | 0.046 | −98% ❗ |
| Oct | 0.653 | 0.202 | −69% | 2.080 | 0.014 | −99% ❗ |
| Nov | 0.760 | 0.758 | ~0% | 4.133 | 1.534 | −63% |
| Dec | 0.250 | 0.646 | +158% | 2.075 | 1.821 | −12% |

As presented in Table 4.9, the results reveal a clear and consistent seasonal pattern in low-flow behavior under future climate conditions.

During the winter months, low-flow discharge increases notably at both stations. At the Cene station, Q95 rises from 0.154 $m^3/s$ to 0.656 $m^3/s$ in January (+325%) and from 0.250 $m^3/s$ to 0.646 $m^3/s$ in December (+158%). Similarly, at the Montodine station, Q95 increases from 0.639 $m^3/s$ to 2.374 $m^3/s$ in January (+271%), indicating enhanced water availability during the wet season.

In contrast, a significant reduction in low-flow conditions is observed during spring and summer. At Cene, Q95 declines from 1.937 $m^3/s$ to 0.500 $m^3/s$ in May (−74%) and from 0.942

m³/s to 0.411 m³/s in June (−56%). The most severe decrease occurs in August, where Q95 drops from 0.833 m³/s to 0.092 m³/s (−89%), indicating intensified low-flow conditions.

The downstream station (Montodine) shows even more pronounced changes. In August, Q95 decreases dramatically from 2.442 m³/s to 0.007 m³/s (−99%), while September and October also exhibit extreme reductions exceeding −98%. These results indicate near-zero discharge conditions and a significantly increased risk of hydrological drought in the downstream section of the basin.

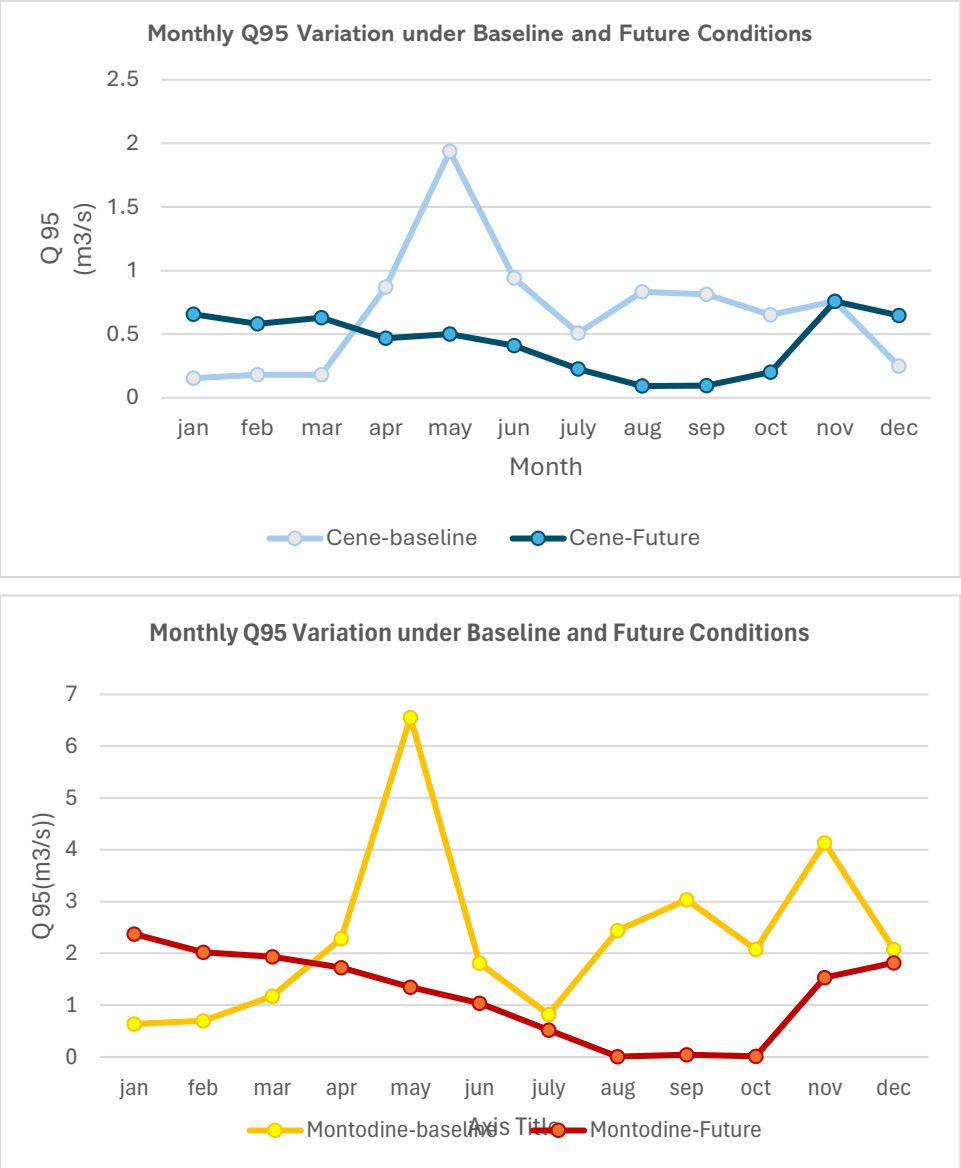


*Figura 4.5Monthly variation of Q95 under baseline and future conditions at (a) Cene and (b) Montodine stations.*

The graphical results further emphasize the seasonal contrast between baseline and future conditions. Specifically, low-flow conditions become considerably more severe during the dry season, while an increase in discharge is observed during winter months.

Overall, the findings indicate that climate change leads to a redistribution of water availability throughout the year, intensifying drought conditions in summer and shifting flow regimes toward higher winter discharge.

### *4.6.2 Annual Low-Flow Variability*

To further investigate temporal variability, annual Q95 values were calculated for both baseline (2014–2025) and future (2026–2050) periods.

The complete annual Q95 dataset is provided in Appendix E.

As presented in the detailed dataset, the baseline period exhibits moderate interannual variability. At the Cene station, Q95 values range between approximately **0.155 m³/s and 1.064 m³/s**, indicating relatively stable low-flow conditions during the historical period.

However, under future climate conditions, substantially higher variability is observed. For example, Q95 decreases to extremely low values such as **0.008 m³/s in 2046**, indicating near-zero discharge conditions. At the same time, higher values are observed in certain years, such as **1.068 m³/s in 2037**, reflecting pronounced interannual fluctuations.

A similar pattern is observed at the Montodine station, where extreme low-flow conditions occur in years such as **2035 (0.01 m³/s)** and **2046 (0.0003 m³/s)**. These extremely low values indicate severe hydrological drought conditions and highlight the increased vulnerability of the downstream section of the basin.

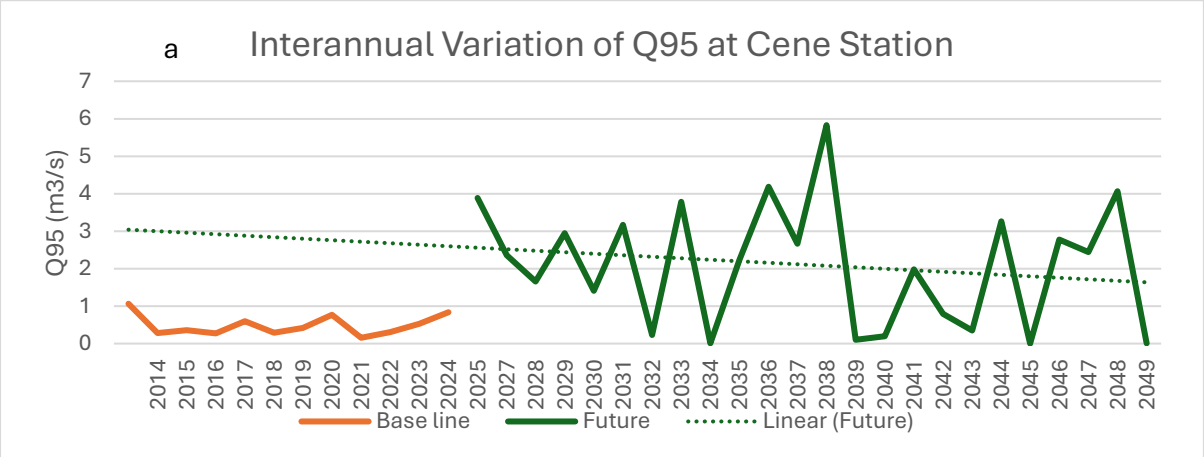

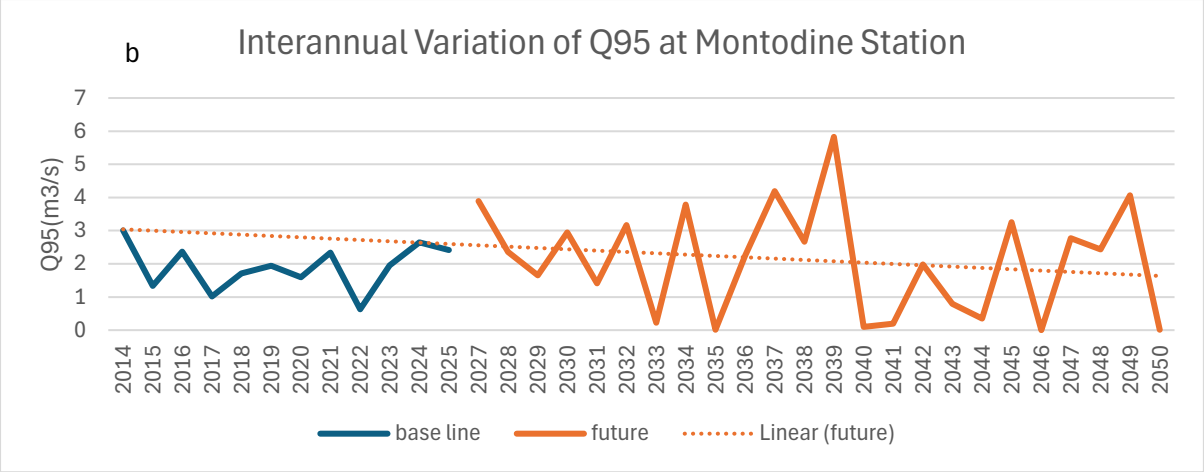


*Figure 4.6Interannual variation of Q95 under baseline and future conditions at (a) Cene and (b) Montodine stations.*

The graphical results further emphasize the increased variability of low-flow conditions under future scenarios. Compared to the baseline period, the frequency of extreme low-flow years is significantly higher in the future.

Overall, the results indicate that climate change affects not only the magnitude of low flows but also enhances interannual variability, leading to more frequent and severe drought events.

### *4.6.3 Discussion of Results*

The combined analysis of monthly and annual Q95 indices highlights a clear spatial variability in the response of low-flow conditions to climate change across the Serio River basin.

The upstream station (Cene) shows moderate changes, with increased winter discharge and reduced flows during the dry season. In contrast, the downstream station (Montodine) exhibits more pronounced reductions, particularly during summer, where Q95 values approach near-zero conditions, indicating higher vulnerability to hydrological drought.

In addition, future conditions are characterized by increased interannual variability, with more frequent occurrences of extremely low-flow years. This suggests a less stable hydrological regime and greater uncertainty in water availability.

Overall, the results indicate that climate change affects not only the magnitude of low flows but also their seasonal distribution and variability, which should be considered in future water resource management.

# 5 Chapter 5: CONCLUSIONS

This study investigated the impacts of climate change on river discharge and low-flow conditions in the Serio River basin using the SWAT+ hydrological model. Climate projections under the RCP4.5 scenario were bias-corrected and applied to simulate future hydrological conditions (2027–2050), which were then compared with the baseline period (2014–2025). Model calibration and validation were performed using observed discharge data to ensure reliable simulation of basin-scale hydrological processes. Low-flow conditions were assessed using the Q95 index.

Calibration significantly improved model performance at the basin outlet (Channel 01), with KGE increasing to 0.75 and NSE to 0.56, indicating acceptable simulation of discharge dynamics. Validation results confirmed stable predictive capability. Performance at the upstream station (Channel 12) remained weaker, highlighting spatial variability and the limitations of single-point calibration.

Copernicus climate data exhibited systematic underestimation of precipitation (−27% to −42%) and temperature magnitude, despite reasonable correlation for temperature. This confirms that large-scale bias correction does not fully remove local-scale errors, particularly for precipitation, which was identified as the dominant source of uncertainty.

Future projections indicate a consistent warming trend across the basin (+0.21°C to +0.42°C annually), with stronger increases in summer and autumn. Precipitation shows an overall decrease (−3.7% to −9.6%), with pronounced reductions in autumn and winter ‹and slight increases in spring. These seasonal shifts are critical for hydrological response.

A substantial reduction in river discharge is projected under future climate conditions. At the upstream station (Cene), discharge decreases by approximately −72.7%, while at the downstream station (Montodine), reductions reach −26.3%. The most significant decreases occur during summer, indicating increased water stress during dry periods.

Low-flow analysis revealed spatially variable responses. At the upstream station (Cene), low-flow conditions show moderate seasonal changes, with increases during winter and substantial reductions during the dry season.

In contrast, the downstream station (Montodine) shows significant deterioration, particularly during summer, where Q95 values approach near-zero conditions. These results indicate a substantial decline in minimum flow conditions in the lower basin.

The combined effects of increasing temperature and decreasing precipitation lead to enhanced evapotranspiration and reduced effective runoff, which in turn intensifies low-flow conditions. The stronger impact observed at the downstream station suggests that cumulative basin processes and reduced upstream contributions amplify low-flow severity along the river. Seasonal shifts, particularly reduced autumn and winter precipitation, further limit groundwater recharge, contributing to reduced baseflow during dry periods.

Several limitations should be acknowledged. First, uncertainties associated with climate projections and downscaling methods may affect the accuracy of future simulations. Second, precipitation bias remains a major source of uncertainty despite correction. Third, calibration was primarily based on a single outlet station, which may not fully capture spatial variability across the basin. Finally, model simplifications and data limitations may influence the representation of groundwater processes and low-flow dynamics.

Future studies should consider multiple climate scenarios (e.g., RCP8.5) to better capture the range of possible hydrological responses. Incorporating multi-model ensembles and alternative hydrological models could improve robustness. Further investigation of seasonal low-flow dynamics and groundwater processes is recommended. In addition, more detailed calibration at multiple stations could enhance spatial accuracy. Finally, the integration of water management strategies and adaptation measures should be explored to mitigate projected reductions in water availability.

# Bibliography

[1] G. Feulner, “Global Challenges: Climate Change,” *Glob. Chall.*, vol. 1, no. 1, pp. 5–6, Sep. 2015, doi: 10.1002/gch2.1003.

[2] Z. W. Kundzewicz, “Climate change impacts on the hydrological cycle,” *Ecohydrol. Hydrobiol.*, vol. 8, no. 2–4, pp. 195–203, 2008.

[3] M. Rahman, T. Bolisetti, and R. Balachandar, “Effect of climate change on low-flow conditions in the Ruscom River watershed, Ontario,” *Trans. ASABE*, vol. 53, no. 5, pp. 1521–1532, 2010.

[4] A. K. Gain, W. W. Immerzeel, F. C. Sperna Weiland, and M. F. P. Bierkens, “Impact of climate change on the stream flow of the lower Brahmaputra: trends in high and low flows based on discharge-weighted ensemble modelling,” *Hydrol. Earth Syst. Sci.*, vol. 15, no. 5, pp. 1537–1545, 2011.

[5] M. Abbas, L. Zhao, and Y. Wang, “Perspective impact on water environment and hydrological regime owing to climate change: A review,” *Hydrology*, vol. 9, no. 11, p. 203, 2022.

[6] R. L. Wilby and I. Harris, “A framework for assessing uncertainties in climate change impacts: Low-flow scenarios for the River Thames, UK,” *Water Resour. Res.*, vol. 42, no. 2, p. 2005WR004065, Feb. 2006, doi: 10.1029/2005WR004065.

[7] K. Sapač, A. Medved, S. Rusjan, and N. Bezak, “Investigation of low-and high-flow characteristics of karst catchments under climate change,” *Water*, vol. 11, no. 5, p. 925, 2019.

[8] V. U. Smakhtin, “Low flow hydrology: a review,” *J. Hydrol.*, vol. 240, no. 3, pp. 147–186, Jan. 2001, doi: 10.1016/S0022-1694(00)00340-1.

[9] T. Tokarczyk, “Classification of low flow and hydrological drought for a river basin,” *Acta Geophys.*, vol. 61, no. 2, pp. 404–421, Apr. 2013, doi: 10.2478/s11600-012-0082-0.

[10] K. Yu, L. Xiong, P. Li, Z. Li, X. Zhang, and Q. Sun, “Analyzing the Impacts of Climatic and Physiographic Factors on Low Flow Distributions,” *Water Resour. Manag.*, vol. 32, no. 3, pp. 881–896, Feb. 2018, doi: 10.1007/s11269-017-1844-x.

[11] M. C. Demirel, M. J. Booij, and A. Y. Hoekstra, “Impacts of climate change on the seasonality of low flows in 134 catchments in the River Rhine basin using an ensemble of bias-corrected regional climate simulations,” *Hydrol. Earth Syst. Sci.*, vol. 17, no. 10, pp. 4241–4257, 2013.

[12] A. L. Kay, A. Griffin, A. C. Rudd, R. M. Chapman, V. A. Bell, and N. W. Arnell, “Climate change effects on indicators of high and low river flow across Great Britain,” *Adv. Water Resour.*, vol. 151, p. 103909, 2021.

[13] M. J. M. De Wit, B. Van Den Hurk, P. M. M. Warmerdam, P. J. J. F. Torfs, E. Roulin, and W. P. A. Van Deursen, “Impact of climate change on low-flows in the river Meuse,” *Clim. Change*, vol. 82, no. 3–4, pp. 351–372, Jun. 2007, doi: 10.1007/s10584-006-9195-2.

[14] A. Alodah and O. Seidou, “Assessment of climate change impacts on extreme high and low flows: an improved bottom-up approach. Water 11: 1236.” 2019.

[15] C. Schneider, C. L. R. Laizé, M. C. Acreman, and M. Flörke, “How will climate change modify river flow regimes in Europe?,” *Hydrol. Earth Syst. Sci.*, vol. 17, no. 1, pp. 325–339, 2013.

[16] K. Yu, L. Xiong, P. Li, Z. Li, X. Zhang, and Q. Sun, “Analyzing the Impacts of Climatic and Physiographic Factors on Low Flow Distributions,” *Water Resour. Manag.*, vol. 32, no. 3, pp. 881–896, Feb. 2018, doi: 10.1007/s11269-017-1844-x.

[17] L. D. O. Serrano, R. B. Ribeiro, A. C. Borges, and F. F. Pruski, “Low-Flow Seasonality and Effects on Water Availability throughout the River Network,” *Water Resour. Manag.*, vol. 34, no. 4, pp. 1289–1304, Mar. 2020, doi: 10.1007/s11269-020-02499-3.

[18] R. L. Wilby and I. Harris, “A framework for assessing uncertainties in climate change impacts: Low-flow scenarios for the River Thames, UK,” *Water Resour. Res.*, vol. 42, no. 2, p. 2005WR004065, Feb. 2006, doi: 10.1029/2005WR004065.

[19] M. Marquès, R. F. Bangash, V. Kumar, R. Sharp, and M. Schuhmacher, “The impact of climate change on water provision under a low flow regime: A case study of the ecosystems services in the Francoli river basin,” *J. Hazard. Mater.*, vol. 263, pp. 224–232, 2013.

# List of Tables

# List of Figures

# Appendices

## Appendix A.Climate Data and Bias Correction Factors

*Table 5-1Monthly precipitation bias correction factors*

| Month | Valbondione | Gandellino | Ardesio | Casnigo |
|---|---|---|---|---|
| Jan | 1.408307 | 1.244308 | 1.438792 | 1.093106 |
| Feb | 2.907101 | 2.410555 | 2.852675 | 2.364534 |
| Mar | 1.579247 | 1.39453 | 1.732076 | 1.351139 |
| Apr | 1.599777 | 1.423285 | 1.964724 | 1.414756 |
| May | 1.570752 | 1.443712 | 2.199548 | 1.691894 |
| Jun | 1.503843 | 1.463383 | 1.858347 | 1.406443 |
| Jul | 1.612289 | 1.404162 | 1.87517 | 1.654852 |
| Aug | 1.290966 | 1.243484 | 1.706332 | 1.534595 |
| Sep | 1.372341 | 1.274822 | 1.725875 | 1.175287 |
| Oct | 1.448382 | 1.124359 | 1.607212 | 0.866368 |
| Nov | 1.592591 | 1.322518 | 2.138409 | 1.249158 |
| Dec | 1.127179 | 0.961642 | 1.265655 | 0.900784 |

*Table 5-2.Monthly temperature bias correction factors (°C)*

| Month | Valbondione | Gandellino | Ardesio | Casnigo |
|---|---|---|---|---|
| Jan | 2.85 | 4.02 | 2.6 | 0.96 |
| Feb | 3.94 | 4.82 | 3.11 | 1.7 |
| Mar | 1.46 | 4.6 | 3.01 | 1.23 |
| Apr | 1.16 | 4.85 | 3.2 | 1.59 |
| May | 0.3 | 3.97 | 2.35 | 0.83 |
| Jun | 1.78 | 4.97 | 3.72 | 1.85 |
| Jul | 0.77 | 3.72 | 2.52 | 1.03 |
| Aug | 1.7 | 4.35 | 3.13 | 1.57 |
| Sep | 1.5 | 4.31 | 2.84 | 1.28 |
| Oct | 1.95 | 4.23 | 2.68 | 1.33 |
| Nov | 3.37 | 4.72 | 3.08 | 1.8 |
| Dec | 4.47 | 4.87 | 4.01 | 1.95 |

# Appendix B. Projected Temperature Changes

*Table B.1. Annual and seasonal temperature changes (ΔT = Future − Baseline) at **Valbondione***

| Period / Season | Baseline Temperature (2014–2025) °C | Future .Temperature (2027–2050) °C | ΔT (°C) |
|---|---|---|---|
| Annual | 5.99 | 6.41 | 0.42 |
| Winter (DJF) | -0.29 | -0.23 | 0.06 |
| Spring (MAM) | 7.83 | 8.43 | 0.60 |
| Summer (JJA) | 12.90 | 13.40 | 0.41 |
| Autumn (SON) | 3.37 | 3.92 | 0.56 |

## Gandelino

*Table B.2. Annual and seasonal temperature changes (ΔT = Future − Baseline) at Gandelino*

| Period / Season | Baseline Temperature (2014–2025) °C | Future Temperature (2027–2050) °C | ΔT (°C) |
|---|---|---|---|
| Annual | 9.73 | 10.1 | 0.37 |
| Winter (DJF) | 2.18 | 2.77 | 0.59 |
| Spring (MAM) | 12.90 | 13.41 | 0.51 |
| Summer (JJA) | 17.27 | 17.79 | 0.51 |
| Autumn (SON) | 5.70 | 6.29 | 0.59 |

## Ardesio

*Table B.3. Annual and seasonal temperature changes (ΔT = Future − Baseline) at Ardesio*

| Period / Season | Baseline Temperature (2014–2025) °C | Future Temperature (2027–2050) °C | ΔT (°C) |
|---|---|---|---|
| Annual | 9.51 | 9.85 | 0.34 |
| Winter (DJF) | 2.43 | 2.32 | -0.11 |
| Spring (MAM) | 12.72 | 13.19 | 0.47 |
| Summer (JJA) | 17.23 | 17.86 | 0.63 |
| Autumn (SON) | 5.37 | 5.93 | 0.56 |

## Casnigo

*Table B.4. Annual and seasonal temperature changes (ΔT = Future − Baseline) at Casnigo*

| Period / Season | Baseline Temperature (2014–2025) °C | Future Temperature (2027–2050) °C | ΔT (°C) |
|---|---|---|---|
| Annual | 12.27 | 12.48 | 0.21 |
| Winter (DJF) | 4.83 | 4.55 | -0.28 |
| Spring (MAM) | 15.79 | 16.11 | 0.32 |
| Summer (JJA) | 20.48 | 21.02 | 0.54 |
| Autumn (SON) | 7.64 | 8.11 | 0.47 |

# Appendix C. Projected Precipitation Changes

*Table C.1 – Annual and seasonal precipitation changes (ΔP% = percentage change relative to baseline) Valbondione*

| Period / Season | Baseline Precipitation (2014–2025) mm | Future Precipitation (2027–2050) mm | ΔP (%) |
|---|---|---|---|
| **Annual** | 5.73 | 5.52 | -3.66 |
| **Winter (DJF)** | 4.25 | 3.56 | -16.23 |
| **Spring (MAM)** | 5.98 | 6.51 | 9.39 |
| **Summer (JJA)** | 6.33 | 6.36 | -1.57 |
| **Autumn (SON)** | 6.51 | 5.64 | -13.05 |

*Table C.2 – Annual and seasonal precipitation changes (ΔP% = percentage change relative to baseline) Gandelino*

| Period / Season | Baseline Precipitation (2014–2025) mm | Future Precipitation (2027–2050) mm | ΔP (%) |
|---|---|---|---|
| **Annual** | 4.87 | 4.70 | -3.88 |
| **Winter (DJF)** | 3.54 | 3.06 | -12.82 |
| **Spring (MAM)** | 5.11 | 5.61 | 9.78 |
| **Summer (JJA)** | 5.58 | 5.63 | 0.89 |
| **Autumn (SON)** | 5.34 | 4.49 | -16.23 |

## ARDESIO

*Table C.3 – Annual and seasonal precipitation changes (ΔP% = percentage change relative to baseline) Ardesio*

| Period / Season | Baseline Precipitation (2014–2025) mm | Future Precipitation (2027–2050) mm | ΔP (%) |
|---|---|---|---|
| **Annual** | 6.64 | 6.02 | -8.93 |
| **Winter (DJF)** | 3.69 | 3.63 | -2.42 |
| **Spring (MAM)** | 7.5 | 7.29 | -0.13 |
| **Summer (JJA)** | 6.80 | 7.03 | 2.92 |
| **Autumn (SON)** | 8.76 | 6.08 | -30.59 |

CASIGNO

*Table C.4 – Annual and seasonal precipitation changes (ΔP% = percentage change relative to baseline) Casigno*

| Period / Season | Baseline Precipitation (2014–2025) mm | Future Precipitation (2027–2050) mm | ΔP (%) |
|---|---|---|---|
| **Annual** | 4.08 | 3.68 | -9.58 |
| **Winter (DJF)** | 2.77 | 2.61 | -4.39 |
| **Spring (MAM)** | 4.53 | 4.60 | 2.67 |
| **Summer (JJA)** | 5.28 | 4.60 | -13.20 |
| **Autumn (SON)** | 3.77 | 2.90 | -22.4 |

# Appendix D. Projected River Discharge Changes

*Table D.1 – Mean annual and seasonal discharge comparison (Baseline vs Future) Cene*

| Period / Season | Baseline Discharge (2014–2025) m³/s | Future Discharge (2027–2050) m³/s | ΔQ (%) |
|---|---|---|---|
| **Annual** | 19.77 | 5.4 | -72.68 |
| **Winter (DJF)** | 13.62 | 4.68 | -65.63 |
| **Spring (MAM)** | 24.75 | 5.69 | -77.01 |
| **Summer (JJA)** | 18.22 | 4.32 | -76.28 |
| **Autumn (SON)** | 22.63 | 6.9 | -69.5 |

*Table D.2 – Mean annual and seasonal discharge comparison (Baseline vs Future) Montodine*

| Period / Season | Baseline Discharge (2014–2025) m³/s | Future Discharge (2027–2050) m³/s | ΔQ (%) |
|---|---|---|---|
| **Annual** | 17.11 | 12.61 | -26.30 |
| **Winter (DJF)** | 14.54 | 12.32 | -15.26 |
| **Spring (MAM)** | 16.95 | 14.27 | -15.81 |
| **Summer (JJA)** | 13.95 | 9.04 | -35.19 |
| **Autumn (SON)** | 23.43 | 14.82 | -36.80 |

# Appendix E. Detailed Low-Flow Statistics(Q95)

*Table 5.1– Annual Q95 values for baseline periods at Cene and Montodine stations*

| Year | Cene | Montodine |
|---|---|---|
| 2014 | 1.064 | 3.0074 |
| 2015 | 0.28146 | 1.3292 |
| 2016 | 0.35875 | 2.3675 |
| 2017 | 0.27606 | 1.0138 |
| 2018 | 0.5939 | 1.7106 |
| 2019 | 0.29372 | 1.9394 |
| 2020 | 0.42205 | 1.59575 |
| 2021 | 0.7658 | 2.336 |
| 2022 | 0.15502 | 0.62836 |
| 2023 | 0.30958 | 1.9564 |
| 2024 | 0.5264 | 2.64575 |
| 2025 | 0.83692 | 2.4128 |

*Table E.2– Annual Q95 values for future  periods at Cene and Montodine stations*

| Year | Cene | Montodine |
|---|---|---|
| 2027 | 0.90184 | 3.8902 |
| 2028 | 0.6643 | 2.35675 |

| Year | Cene | Montodine |
|---|---|---|
| 2029 | 0.56906 | 1.6526 |
| 2030 | 0.62192 | 2.9446 |
| 2031 | 0.42184 | 1.4068 |
| 2032 | 0.82655 | 3.1675 |
| 2033 | 0.31484 | 0.22668 |
| 2034 | 1.0466 | 3.7838 |
| 2035 | 0.18224 | 0.0101972 |
| 2036 | 0.683775 | 2.23525 |
| 2037 | 1.0686 | 4.1868 |
| 2038 | 0.5617 | 2.6642 |
| 2039 | 0.99158 | 5.829 |
| 2040 | 0.165275 | 0.100145 |
| 2041 | 0.20798 | 0.1986 |
| 2042 | 0.86488 | 1.9844 |
| 2043 | 0.52348 | 0.78996 |
| 2044 | 0.269025 | 0.346025 |
| 2045 | 0.78886 | 3.2594 |
| 2046 | 0.0082652 | 0.0003295 |
| 2047 | 0.8264 | 2.777 |
| 2048 | 0.709975 | 2.43875 |
| 2049 | 0.9316 | 4.0662 |
| 2050 | 0.088104 | 0.0068458 |